STEERABLE ANTENNA ARRAY FOR UAV APPLICATIONS

by

VARSHA VIJAYKUMAR

THESIS

Submitted in partial fulfillment of the requirements
for the degree of Master of Science
in Electrical Engineering
at
The University of Texas at Arlington
December 2017

ACKNOWLEDGEMENTS

I would like to sincerely thank Dr. Jonathan W. Bredow for giving me the opportunity to do thesis under him, and for his constant guidance and insights throughout this thesis.

I would thank Dr. Saibun Tjuatja and Dr. Jung-Chih Chiao for taking time and agreeing to be a part of thesis defense committee.

I am thankful to Todd Kelley for helping with antenna milling as well as for constantly providing access to UTA Markers Space to use ANSYS HFSS.

Also, I thank my parents and my friends at UTA for supporting throughout this thesis. Finally, thanks to all the teachers who have been an inspiration for building interest in me, towards electromagnetics and antenna subjects.

ABSTRACT

Steerable Antenna Array for UAV Applications

Varsha VijayKumar, MS

The University of Texas at Arlington, 2017

Supervising Professor: Jonathan W. Bredow

An antenna array system design, demonstrating the possible application on an unmanned aerial vehicle platform using a full wave electromagnetic simulation software is presented. Linear array of patches in E plane and H plane are designed consisting of 4 elements with a beam steering ability of ±40 degree from the broadside direction with a peak gain of 12.23dB. Further an arrangement illustrating four such linear arrays, that can switch between each other to cover the entire azimuth scanning is shown. After a series of modified patch antenna designs with an attempt to increase the gain, an inset fed microstrip patch antenna is chosen as a basic radiating element considering its design simplicity and efficient radiation characteristics owing to the limited dimension available on a UAV platform. Gain of a single element inset fed patch antenna is found to be 7.2 dB resonating at 5.6GHz with 10dB bandwidth range of 190MHz.The dimension of a single patch is $0.3\lambda_0 \times 0.28\lambda_0 \times 0.02\ \lambda_0$. Also, a single element patch antenna is fabricated with the help of a milling machine and analyzed using a vector network analyzer.

Table of Contents

Chapter 1

1.1 Introduction

Unmanned aerial vehicles are aerial platforms without a human pilot on board. They are helpful for operating in dangerous environments which are high-risk for human intervention [1]. UAV's are used in various sectors such as science, civilian and military. Cluster of UAVs are currently taking over single UAV operation to cover larger geographical area with high speed data acquisition in case of remote sensing applications including geographical data observation, soil monitoring and precision agriculture. Also, they find major application in disaster management systems. In the absence of a communication network infrastructure in case of a disaster scenario, providing on demand communication is a requirement. Efficient and coordinated aerial communication between UAVs is a necessity in creating a backhaul on demand communication infrastructure. UAVs can communicate between each other in an unlicensed higher frequency bands (Wi-Fi 2.4 / 5 GHz). An uninterrupted communication covering long range with minimal interference between UAV and UAV in the air is a prerequisite to have stable backhaul network. From Friis Transmission equation, it is evident that, to have an increased RX sensitivity, without increasing TX power, high gain point to point communication is required. Hence, directional antennae play a major role to cater to the requirements mentioned above [2]. Additionally, a phased array antenna system with beam steering ability covering the azimuth range to establish a communication link, based on the positioning information of UAVs aids to robust the system design. This helps to reduce the slow response caused by mechanical control.

1.2 Literature Review

The following papers elucidates the brief overview on the study done with respect to explore the research carried out in phased array antenna system design

Wide angle scanning Phased array antenna

This paper [3] provides the design of a magnetic microstrip patch dipole antenna used in phased array with wide beam scanning range of $\pm 76^{\circ}$ and $\pm 64^{\circ}$ in both E and H plane respectively. The overall gain fluctuates within 3dB in the complete scan range. With a view to enhance the HPBW (Half Power Beam Width) to have larger scanning angles several antenna designs are revisited in this paper. The authors provide a brief description of the antennas visited and their difficulties in achieving the required radiation characteristics owing to the design requirements and constraints. The antennas discussed are

a) high profile pattern-reconfigurable antennas in which there are printed strips loaded with switches or pin-diodes at quarter wavelength, from this design a higher beam width is achieved but it is unsuitable for low profile systems.

b) To reduce the profile of the antenna array, artificial magnetic conductor formed by metasurface is mentioned. The disadvantage is that the metasurfaces are difficult to design and have very narrow bandwidth.

c) Slot antennas (magnetic dipoles) which can give omnidirectional radiation characteristics when placed near electric conductors, but are not preferred due to bulky structure.

d) Microstrip magnetic dipoles, that have larger dimension in one plane making it unsuitable to scan in that plane.

Considering the above-mentioned points, this paper proposes a novel magnetic dipole antenna with wide angle scanning and low profile with overall dimension of $0.32\lambda_0 \times 0.32\lambda_0 \times 0.03\lambda 0$. The E and H plane array mentioned in this paper has nine elements giving overall gain of 13.4 dB. The antenna size approximates to that of a conventional patch. antenna. The bandwidth of the proposed antenna is slightly higher than patch antenna. The antenna is designed in HFSS with an infinite ground plane. For practical purpose, the fabricated antenna is designed upon a large ground plane. The length of the proposed array of nine antenna elements is around 16cm and overall length would be larger in size due to large ground plane structure to maintain omnidirectional radiation characteristics. From this paper one can infer that such an array may be unsuitable for applications that require smaller sized platforms.

Antenna Arrays for Unmanned Aerial Vehicle

This paper [4] presents two antenna solutions for an Unmanned Aerial Vehicle (UAV), where the available space for the antenna in the UAV has a cylindrical form. These antennas operate at 2.4GHz frequency band. The designed antennas are composed by a circular array of four elements conformed to cylindrical shape. A rectangular microstrip patch antenna and a PIFA antenna have been selected as basic the radiating elements of each array. The radiation pattern has approximately omnidirectional behavior for both arrays. The design considers the available space due to the geometric dimensions and the required radiation pattern. Paper mentions that, considering the place where the antenna will be located and the required radiation pattern, a rectangular microstrip patch is chosen, though its radiation pattern is not omnidirectional. A circular array antenna must be designed to achieve an omnidirectional pattern. To get a good performance, the minimum number of equally spaced patches are four. Here, each array element is fed by the individual

coaxial port. The antenna has been optimized to work at 2.45 GHz with a bandwidth better than 100 MHz to ensure the coverage of Wi-Fi service. Quite omnidirectional behavior is observed in the paper, when all ports are fed. To obtain the radiation patterns, each patch has been fed with equal amplitude and phase. Among the two illustrations of simulation (microstrip patch and PIFA) provided in this paper, rectangular patch array is suitable for large diameter sections, whereas the second design with PIFA antennas is appropriate for small diameter sections. From here, it can be concluded that configuration of this kind helps to have an azimuth coverage for very shot range. As mentioned in this paper, this design is suitable for UAV to ground station communication.

Wide beam tapered slot antenna for wide angle scanning phased array

This paper [5] talks about the design of double layer exponentially tapered slot antenna (DTSA) which is a modification of a Vivaldi antenna, where the disadvantage with respect to larger size is eliminated in a DTSA. It consists of two back to back substrate arrangement, in which one of the substrate is completely etched on the opposite side of the flare, and other substrate consists of strip line feed printed and sandwiched between the two substrates containing the flares. The substrate material used is RT duroid. It involves the solution of three matching problems, one with the strip line-to-slot line feed transition, second is strip line/CPW transition and third notch-to-free space transition. The paper shows the design of one dimensional E plane array initially, later 16×16 element array in a triangular grid arrangement, capable of scanning in both E and H plane. The frequency of operation focused in this paper is 10GHz. Scan range of ± 60° in H plane and ± 50° in E plane with 4GHz bandwidth can be achieved by this design. The dimension of single antenna element is 24.1mm × 14.2mm and it has HPBW greater than $\pm 60^{\circ}$ in both E and H plane. The major

drawback is that, it uses as double layer and hence its thickness is increased as well as the overall dimension is larger for the antenna operating at 10GHz. The number of elements used to provide the scan range mentioned is also large.

Steerable metamaterial reflectarray with tunable varactor diodes

This paper [6] discusses on the design of double k-shaped metamaterial 12× 12 array operating in Ku band and illustrates with design simulation that capacitance and series resistance can replace the traditional phase tuning methods. The resonant frequency and phase shift of the reflectarray are dominated by the operating capacitance of the varactor diodes. The varactor diodes are integrated across the gap between the k shaped metamaterial unit cells. The capacitance varies from 0.14 pF to 1.14 pF for the frequency range of 11.5GHz to 12.8GHz and the dynamic range of phase reaches 300°. The beam steering range is up to ±60°. The maximum loss over the entire bandwidth is 2.85 dB. The frequency range investigated here is between 12GHz and 18GHz. The fine alignment of the control voltage for each varactor is critical for the metamaterial reflectarray design. The overall thickness of the reflectarray is less than 2mm. The design is a multilayer structure consisting of 8 layers. To prevent grating lobes and mutual coupling the cell dimension was set to 10mm. The periodic reflectarray consists of individual via in each unit cell to easily control several varactor diodes. When a phase difference is arranged along the E-field direction in the array, the beam can be steered effectively. By adjusting the phase gradient $\Delta\varphi$, the proposed periodic reflectarray can determine the direction of the reflected waves. The drawback of the investigated array structure for the present application is that, the array uses 144-unit cells to scan the beam $\pm 60^{0}$ also it requires multilayer configuration.

Planar Dual-Band Wide-Scan Phased Array

Here [7] comb slot loaded patch antenna capable of operating in dual bands (8.25GHz and 11GHz) with a frequency ratio of 1.4:1 is designed. The feeding structure of the antenna is responsible for good bandwidth in both the bands. The bandwidth of the antenna is about 580MHz and 990MHz in low and high bands respectively. The antenna maintains consistent radiation pattern and can be steered in both E and H plane upto 60° in low band and 50° in high band. This antenna design supports both electric and magnetic radiation characteristics. The magnetic radiation is achieved by the addition of 4 arm comb shaped slots to patch antenna. The patch antenna is an electric radiator. The shape and size of both electric and magnetic radiators are selected to achieve dual band operation. The feeding structure is designed such that there is simultaneous excitation of both magnetic and electric radiators. It is a modified L probe feed with a capacitive matching ring. It consists of plate through hole cylinder (PTH), matching ring and a stripline transition. The stripline transition is separated from patch by a dielectric layer which excites the comb-slot giving rise to magnetic radiations. This feeding mechanism achieves wide scanning and bandwidth properties. The only drawback of this antenna for a potential UAV array is the substrate thickness, which is 4.2mm.

1.3 Design Requirements and thesis outline

Friis transmission equation can be a good starting point to begin the analysis on the design requirements. For a Line of Sight (LOS) case, equation 1 is used to find the received power, given the transmit power, gain of the transmit and receive antenna and the distance between the antennas.

$$P_R = \frac{P_T G_T G_R c^2}{\left(4\pi R f\right)^2} \qquad \text{Equation 1}$$

From the typical UAV specifications, the transmit power is not more than 20dBm and receiver sensitivity is greater than -90dBm [12]. For a UAV operating at 5.8GHz frequency, with transmit power of 13dBm and receiver sensitivity of 90dBm, to have a communication range of 5km, the receiver and transmitter antenna gain should be 9.192 dB. This is assuming LOS communication with same receive and transmit antennas used. Here, minimum values of transmit power and receiver sensitivity are chosen, so that maximum possible gain can be calculated for LOS case. Considering the above-mentioned explanation, to have an interrupted 5km range of communication, the antenna gain should possibly be as high as 9dB, in the worst-case scenario, taking into account additional losses that can be incurred in a real measurement condition. Therefore, the following requirements are outlined.

a.) The antenna array design should have gain more than 10 dB, the gain must not fall below 10 dB value during the scanning range. This ensures to have long range communication.

b.) The number of elements used to form an array should be minimal, considering the limited space available.

c.) The radiation characteristics should be standard broadside or end fire which gives an easier reference point for scanning.

d.) The antenna element must be low profile, owing to the size, weight and aerodynamic drag limitations.

e.) A convenient system design which can cover the entire azimuth scan electrically, to ensure reliable communication link.

Considering, the mentioned design constraints, the thesis report is outlined as following chapters to achieve the necessary criteria. Chapter 2 gives an overview of the microstrip patch antennas. Chapter 3 talks about antenna arrays. Chapter 4 provides detailing about the various designs considered including the array design, as well as the system design required to achieve the demands mentioned. It also shows the single element antenna fabrication and analysis result. Chapter 5 gives the summary and discusses the future work.

Chapter 2

2.1 Microstrip Patch Antennas

Microstrip patch antennas are low profile, simple, conformable, inexpensive to manufacture, mechanically robust, compatible with MMIC designs. They are versatile in terms of resonant frequency, polarization and impedance. The disadvantages are low efficiency, poor polarization, poor scanning range, narrow bandwidth and spurious radiations from feed lines. Increasing the thickness of the substrate can extend the efficiency (provided surface waves are absent) and bandwidth. But, as the thickness increases, surface waves are introduced which are not desirable, because they extract power from the total available for direct radiation (space waves). The surface waves are scattered at bends and surface discontinuities and degrade the antenna pattern and polarization. Surface waves can be eliminated, along with maintaining large bandwidths, by using cavities, stacking patches etc. [8]

Microstrip patch antenna radiates in broadside direction that is normal to the surface of the patch. End fire radiation can also be obtained by proper mode selection. Thick substrates with low dielectric constants provide better efficiency with larger bandwidth but at the cost of larger size of the antenna element. Thin substrates with high dielectric constant are used in microwave circuitry, at the expense of narrow bandwidth and low efficiency. [8]

2.1.1 Feeding Methods for Patch antennas

Most common feeding techniques for feeding microstrip patch antennas are a.) Microstrip line feed b.) Proximity coupling feed c.) Aperture coupling feed d.) Coaxial probe feed

Microstrip feed line is a conducting strip, whose width is smaller to the patch. They are easy to fabricate and simple to match by just adjusting the feed position or the inset position. But as the substrate thickness increases, surface waves and spurious feed radiation increase, which degrades the bandwidth [8]. Feeding the antenna at the edge yields a high input impedance, which is minimized by inset feeding. Current is low at the ends of a half-wave wavelength patch and increases in magnitude toward the center, the voltage follows a reverse profile. The input impedance Z=V/I is zero at the center of the patch and hence the impedance can be reduced by feeding the patch towards the center. The current follows a sinusoidal distribution. That is moving a distance R causes the current to increase by an amount $\cos\left(\text{pi} * \frac{\text{R}}{\text{L}}\right)$, the voltage also decreases by the same amount. The input impedance is given by the equation [9].

$$Z_{in}(R) = \cos^2(\text{pi}*R/L)\ Z_{in}$$ Equation 2.1 [9]

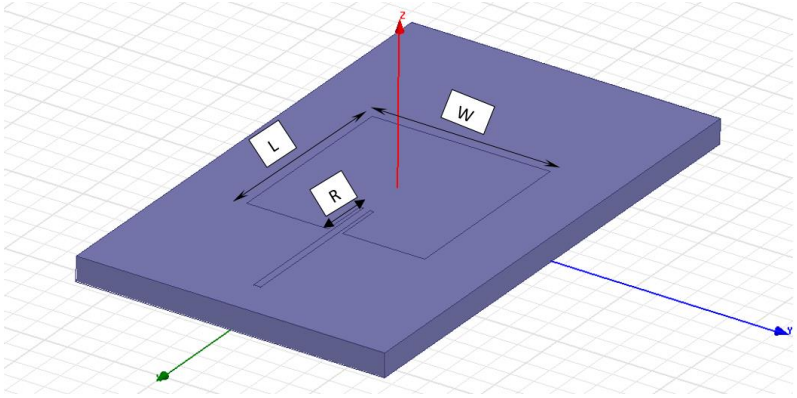

Figure 2.1.1 Inset fed patch antenna

Another technique of microstrip line feeding is, using quarter wavelength transmission line of impedance Z_1 which is matched to input impedance Z_0 of the transmission line. Let Z_A be the input impedance of the antenna, then with a view to match input impedance Z_{in} to the transmission line impedance Z_0, the following equation can be obtained when input impedance is viewed from the beginning of the quarter-wavelength line becomes

$$Z_{in} = Z_0 = Z_1^2 / Z_A$$ Equation 2.2 [9]

The value Z_1 can be altered by changing the width of the quarter wavelength strip. Wider the strip length implies lesser the value of characteristic impedance Z_0 [9]

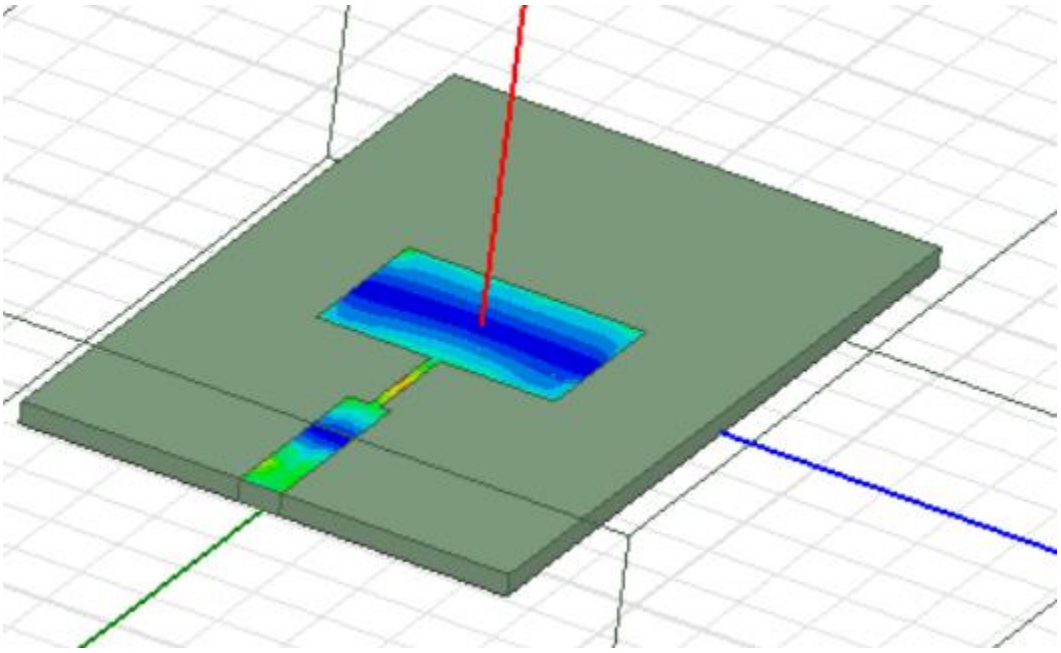

Figure 2.1.2 Quarter wavelength microstrip line feed

In case of coupled feeds, there is no direct contact with the antenna. The gap between the feed and the antenna introduces a capacitive nature [9]. The aperture coupling method consists of two substrates which are separated by a ground plane. On the bottom side of the lower substrate there is a microstrip feed line whose energy is coupled to the patch through

a slot on the ground plane separating the two substrates. Usually, the bottom substrate is of higher dielectric constant than the substrate above which is comparatively thicker with low dielectric constant. The ground plane between the substrate helps in isolation between the feed and the radiating element, with a view to minimizes the interference of spurious radiation which affects the radiation pattern and polarization purity. In this design, the substrate electrical parameters, feed line width, slot size and position are used to optimize the design. The main disadvantage is that fabrication of this antenna is not as simple as a microstrip line feed.

In case of coaxial feeds, the inner conductor of the coax is attached to the radiation patch while the outer conductor is connected to the ground plane. Coaxial probe feed is also easy to fabricate and match, also it has low spurious radiation. However, the bandwidth is narrow and it is more difficult to model, especially for thick substrates. [8]

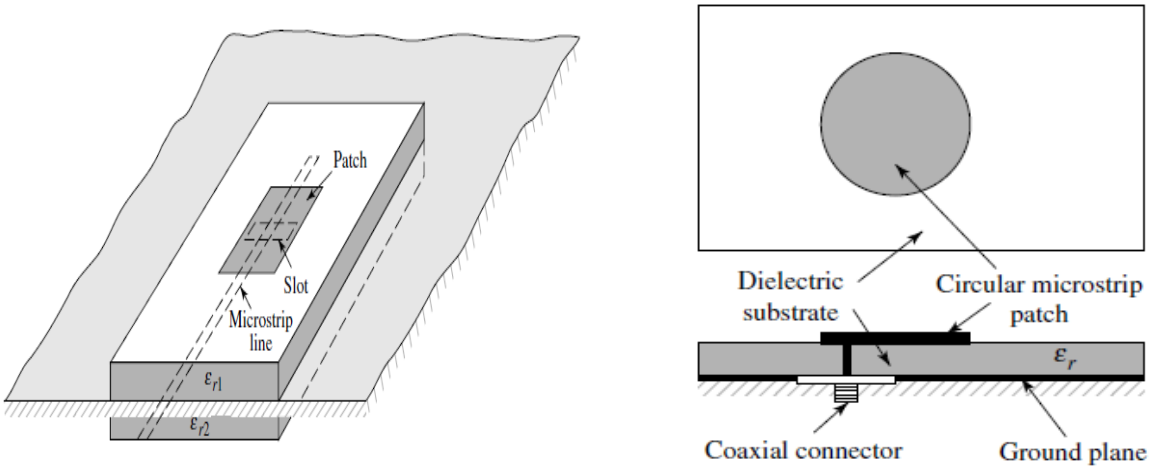

Figure 2.1.3 Aperture coupled patch antenna (left) and coaxial probe feed patch antenna (right) [8]

2.1.2 Design Equation for patch Antenna

Microstrip patch antenna consists of a patch, a feeding element and a ground plane. All of which are high conductive metal. They are placed on top of a dielectric substrate of thickness h and permittivity ε_r. The patch has dimensions of length L and width W [9] The design process starts with specifying resonant frequency, dielectric constant and height h of the substrate, from which width and length of the patch are calculated as follows.

The width of the antenna (radiating edge) plays a major role in determining the radiation characteristics. The wider the width the better the radiation characteristics, but it attains saturation after a certain increase in the width and does not have effect on the radiation pattern. The width of the antenna is given by

$$W = \frac{v_0}{2 f_r} \sqrt{\frac{2}{\zeta_r + 1}} \qquad \text{Equation 2.3 [8]}$$

The length of the microstrip antenna determines the resonant frequency. The expression for length L is given by

$$L = \frac{1}{2 f_r \sqrt{\zeta_{reff}} \sqrt{\zeta_0 \mu_0}} - 2\Delta L \qquad \text{Equation 2.4 [8]}$$

where, ζ_{reff} is the effective dielectric constant given by

$$\zeta_{reff} = \frac{\zeta_r + 1}{2} + \frac{\zeta_r - 1}{2} \left[\sqrt{1 + 12 \frac{h}{W}} \right] \qquad \text{Equation 2.5 [8]}$$

2.1.3 Radiation Mechanism

Fringing effects can help explain the radiation mechanism of a patch antenna. The finite dimensions of the patch antenna, is responsible for the fields to undergo fringing at the edges. The amount of fringing is a function of the dimensions of the patch and the height of the substrate [8]. In case of a patch antenna, since the height of the substrate is very small compared to wavelength of operation, the ratio of length or width to height is very much greater than one, hence fringing effect is very minimal. However, they are required to be taken into consideration, since they affect the resonance frequency. Since some part of the waves travel in dielectric media and some in air, the concept of effective dielectric constant was introduced to account for fringing effects as well as propagation in transmission line. Due to the presence of fringing fields, the resonant frequency shifts to a lesser value and the patch appears electrically larger. Hence, this effect must be introduced in design equation to trim off the extra lengths [9].

The cavity model analysis of the microstrip patch antenna considers dielectric substrates as the cavity bounded by electric conductors from above and below and magnetic conductors along the sides, resembling an open circuit. Since the thickness of the microstrip is usually very small, the waves generated within the substrate undergo considerable reflections when they arrive at the edge of the patch. [8] Hence, only a small amount of the incident wave is radiated. There is formation of sinusoidal standing waves beneath the surface of the patch. Since the height of the substrate is very small, the field variations along the height can be considered constant. Also, since the substrate height is very small, variations along the edges are neglected in this theory. Hence, cavity model considers a perfectly conductive electric

conductor from above and below the substrate and perfect magnetic conductors along the edges, electric field is nearly normal to the surface of the patch. Therefore, only TM^x field configurations will be considered within the cavity for a patch oriented in the y-z plane.

The expressions for the radiated fields in the principle planes given by this theory are as follows [8].

E plane (x-y plane for patch oriented in y-z plane, $\theta = 90^o, 0^o \le \phi \le 90^o \; and \; 270^o \le \phi \le 360^o$) radiation field is given by equation 2.6

$$E_\phi = \frac{+jk_0 W V_0 e^{-jk_0 r}}{\pi r} \left(\frac{\sin\left(\frac{k_0 h}{2}\cos\phi\right)}{\frac{k_0 h}{2}\cos\phi} \right) \cos\left(\frac{k_0 L_e}{2}\sin\varphi\right) \qquad \text{Equation 2.6}$$

H plane (x-z plane for patch oriented in y-z plane, $\phi = 0^o, 0^o \le \theta \le 180^o$) radiation field is given by equation 2.7

$$E_\phi = \frac{+jk_0 W V_0 e^{-jk_0 r}}{\pi r} \left(\sin\theta \frac{\sin\left(\frac{k_0 h}{2}\sin\theta\right)}{\frac{k_0 h}{2}\sin\theta} \frac{\sin\left(\frac{k_0 W}{2}\cos\theta\right)}{\frac{k_0 W}{2}\cos\theta} \right) \qquad \text{Equation 2.7}$$

The radiation pattern in E and H plane using the above equations in MATLAB is given in Figure 2.1.4

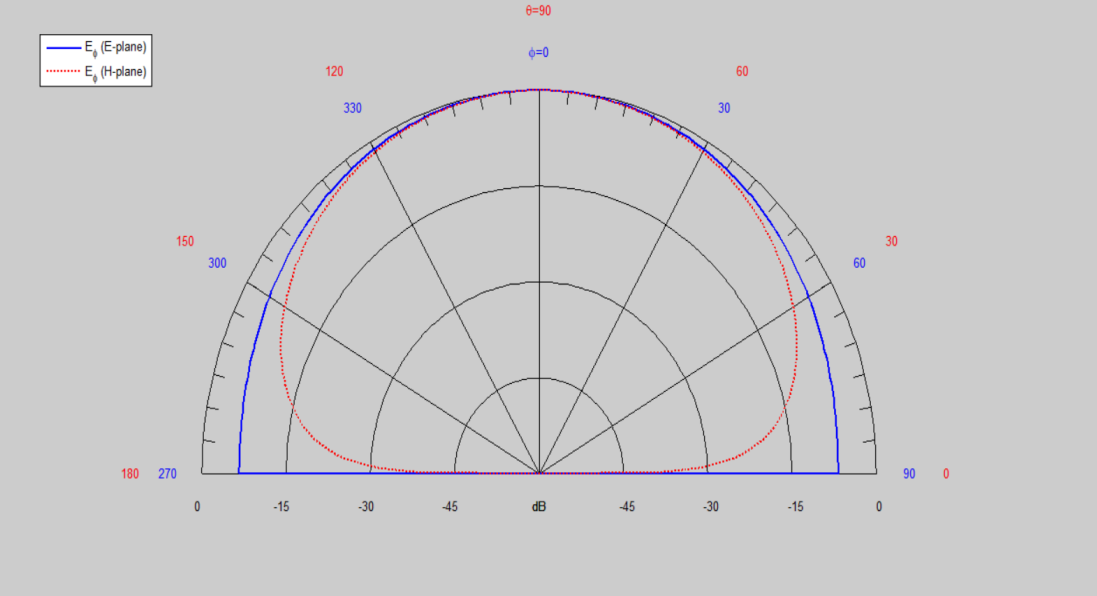

Figure 2.1.4 Normalized Radiation pattern of a patch antenna using cavity model equations in MATLAB

This chapter provides a brief overview about microstrip patch antennas, their working theory with supporting analytical expressions and different feeding methodologies.

Chapter 3

3.1 Antenna Arrays

Antenna arrays are a set of two or more antenna elements. They are processed in such a way as to achieve the required radiation performances. They major advantages of antenna arrays are a.) They provide overall higher gain b.) They are helpful in steering the beam for phased array applications. c.) They are helpful in cancelling out interferences from a particular direction d.) They provide higher SNR [9]. The overall radiation pattern of an antenna array can be controlled by the following five variants [8]

1) Array lattice such as rectangular, triangular, circular, hexagonal etc.
2) Distance between elements in an array
3) Radiation pattern of individual elements
4) Excitation amplitude of the elements
5) Excitation phase of the elements

The Array Factor is a function of the positions of the antennas in the array and the weights used [9]. The overall radiation pattern of the antenna array can be controlled by proper weighting and positioning of the individual elements. The array radiation pattern is the product of radiation due to individual elements multiplied by the array factor, known as pattern multiplication.

E(total) = E (radiation due to individual antenna element) × Array Factor [8]

This chapter gives fundamentals, which are required to be known about antenna arrays. Here, the predominant discussion is on linear arrays, whereas planar arrays are also mentioned.

Uniform Linear Arrays

They consist of N identical antenna elements with equal magnitude of excitation amplitude and progressive phase difference (β) between each element. If the elements in an array are not isotropic sources, the total field can be obtained by multiplying the array factor of the isotropic sources by the field of a single element.

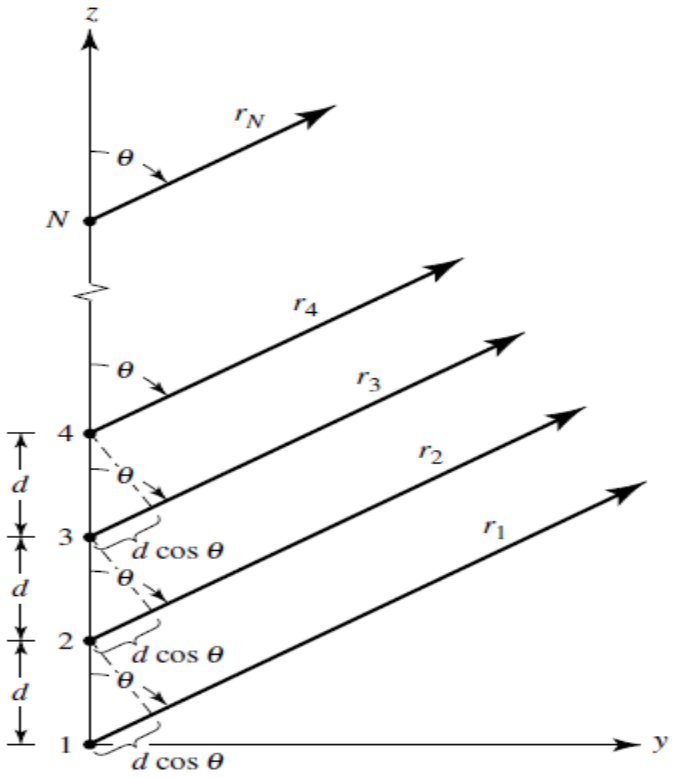

Figure 3.1.1 Uniform N element antenna array geometry along z axis [8]

The array factor expression for isotropic uniform linear array is

$$AF = \sum_{n=1}^{N} e^{j(n-1)\psi}$$

$$\psi = kd\cos\theta + \beta$$

Equation 3.1 [8]

β is the progressive phase difference

Simplifying the above expression gives

$$AF_n = \left(\frac{\sin(\frac{N}{2}\psi)}{(\frac{N}{2}\psi)} \right) \qquad \text{Equation 3.2 [8]}$$

Broadside Radiation Array

In this case the maximum radiation is pointed normal to the axis of the array, that is the maxima of the single element as well as the array is at $\theta_0=90^0$.

The condition for the maxima of the array is $\psi = kd\cos\theta + \beta = 0$, for this to satisfy, we consider $\theta_0=90$ and plug it into equation which gives $\psi = kd\cos\theta + \beta\big|_{\theta=90} = \beta = 0$ [8].This implies that to have a broadside radiation all the uniform identical elements should have equal magnitude and equal phase (that is there should be no phase difference between the elements). Figure 3.1.2. Shows the broadside radiation pattern generated using MATLAB using the above-mentioned equations and conditions for 5 element isotropic array.

End fire Array

In this array the maximum radiation occurs at $\theta_0=0^0$ or 180^0, that is along the axis of the array. The condition for the maxima of the array at $\theta_0=0^0$ is $\psi = kd\cos\theta + \beta\big|_{\theta=0} = kd + \beta \Rightarrow \beta = -kd$ and for $\theta_0=180^0$ the condition is given by $\psi = kd\cos\theta + \beta\big|_{\theta=180} = -kd + \beta \Rightarrow \beta = kd$ [8]. Simulation of end fire array for five isotropic radiators is shown in Figure 3.1.3.

Phased array

The maximum radiation can be scanned in any direction other along with broadside and end fire. Such an antenna array is called scanning array or phased array. The condition for such an array is $\psi = kd\cos\theta + \beta\big|_{\theta=\theta_0} = kd\cos\theta_0 + \beta \Rightarrow \beta = -kd\cos\theta_0$. [8] Figure 3.1.4 shows the array whose main beam points at 60^0

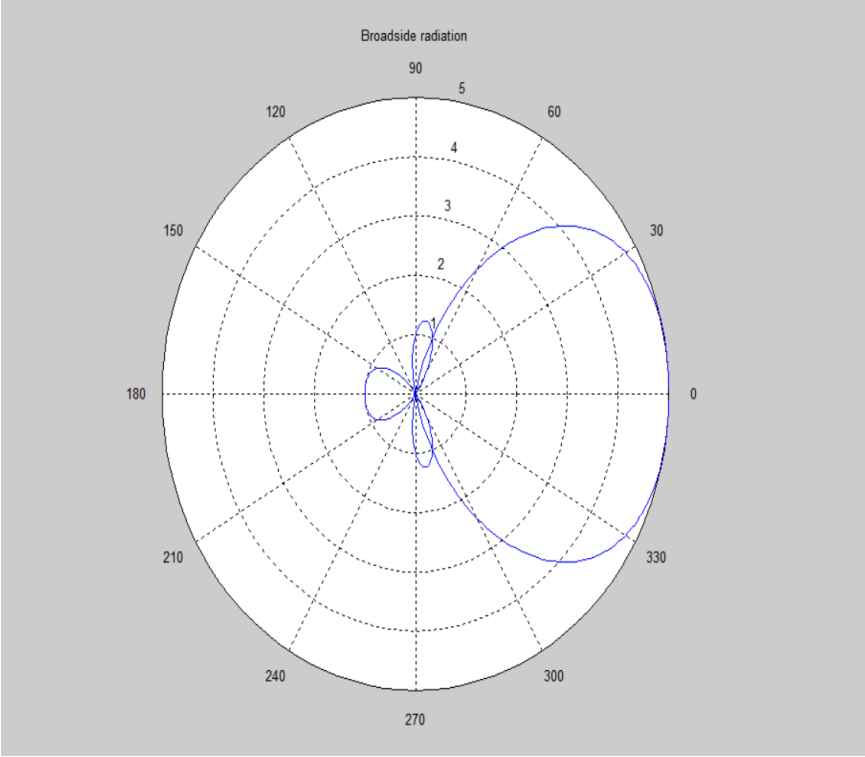

Figure 3.1.2 Broadside array with 5 isotropic radiators

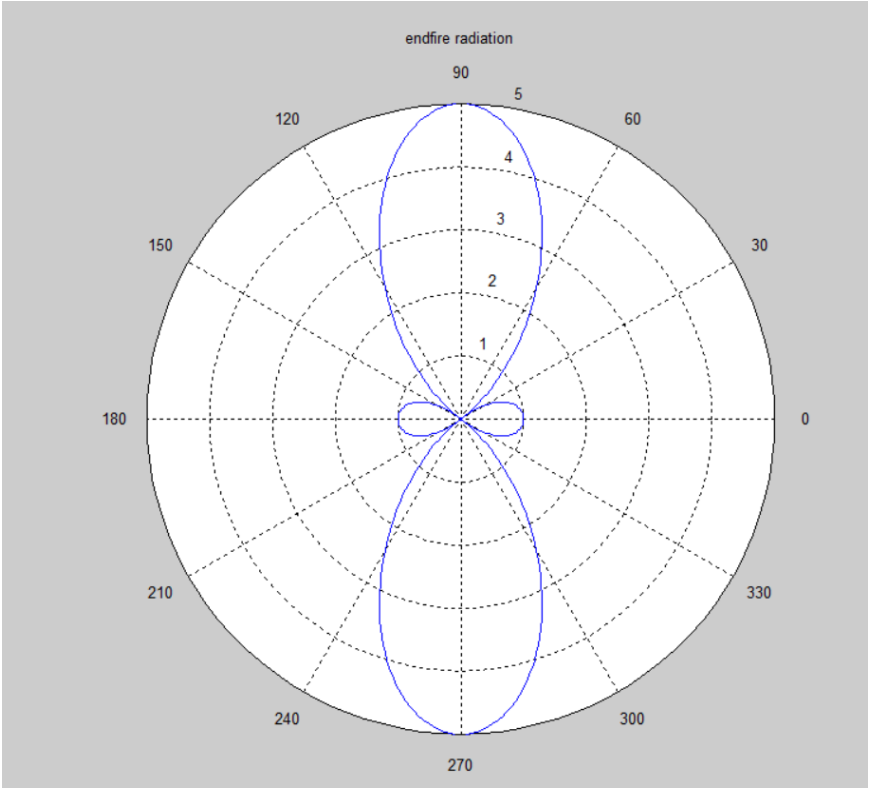

Figure 3.1.3 End fire array with 5 isotropic radiators

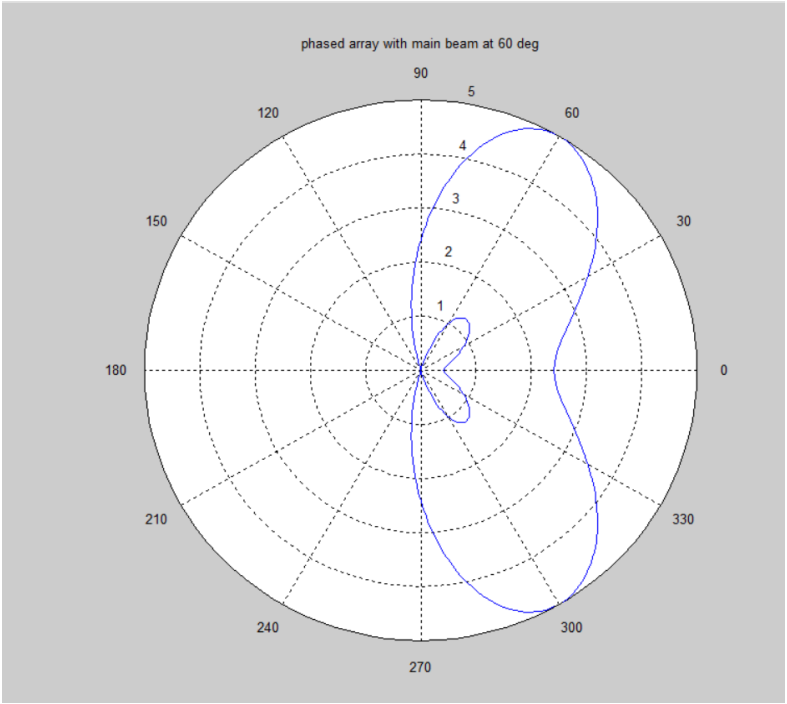

Figure 3.1.4 Phased array of five isotropic radiators with main beam at 60 degrees

It should be noted that in order to eliminate grating lobes the element separation has to be less than half a wavelength.

Planar arrays

They are two dimensional arrays with scanning capability in both the dimensions. They provide larger aperture and higher gain. The total array factor is the multiplication of individual array factor in x and y direction.

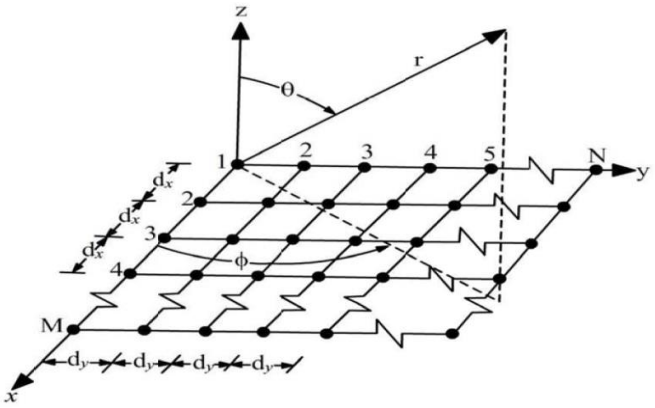

Figure 3.1.5 Planar array geometry [11]

Chapter 4

4.1 Design Approach using Full wave electromagnetic solver (HFSS)

The present aim of the thesis is to, cater to the application of UAV to UAV communication by the design of phased array antenna system. It is carried out using ANSYS HFSS which makes use of Finite Element Method (FEM) to solve the electric field equations. It has adaptive meshing technique which is defined based on the physics of the element, which makes it easier for the user not to pay more attention on the number and size of the meshes. The finite elements are the tetrahedrons. The tool also performs reiterative meshing around the solution frequency, which makes it less prone to error.

Antenna designs which will be described below were performed with an agenda to have an increased gain of the individual antenna, which would be capable to form an array with limited number of elements with better gain and steerability with low fluctuations in gain throughout the scanning range. The aim was to have a slightly greater gain so that the array of such elements can achieve a gain above 10 dB or more with not more than four elements, owing to the size limitations of the platform. Array was designed such that its overall size should not exceed 10cm in length, typically for a 4-element design. Larger gain is responsible to have a long-range communication with low interference among the UAVs in air. Considering the above-mentioned prerequisites, a patch antenna was initially tried, followed by a series of modified patch designs. HFSS simulated results and a brief summary is given for every patch antenna deigns mentioned below.

Patch antenna was chosen as the starting design because of its simple design structure, moderately better gain, low profile, optimum size and fixed analyzable broadside radiation characteristics in the dominant mode.

The very first antenna design implemented was a basic patch antenna with a quarter wavelength transmission line feed. The overall gain of the patch which resonated at 5.1 GHz was found to 3.98 dB. The antenna is fabricated on RT duroid substrate with permittivity ε_r=2.2 with height of 1.6mm. The dimension of the patch is 12.56mm × 17.56mm × 1.6mm The HFSS design layout along with the return loss plot and radiation plots are shown in Figure 4.1.1, 4.1.2 and 4.1.3 respectively.

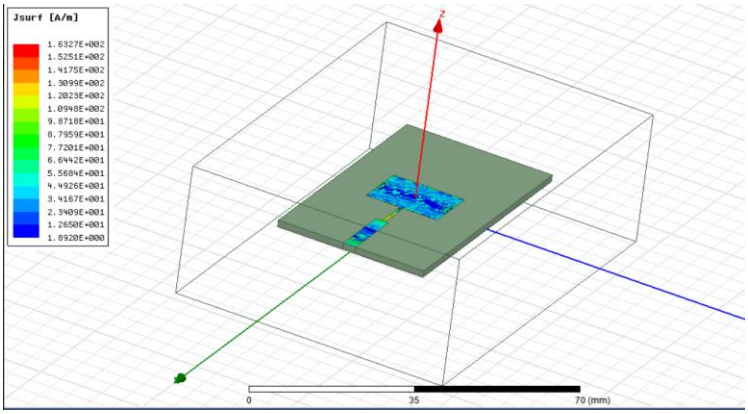

Figure 4.1.1 Quarter wave transmission line feed patch antenna along with current density plot

Figure 4.1.2 3D polar plot of the patch antenna with quarter wavelength transmission line feed

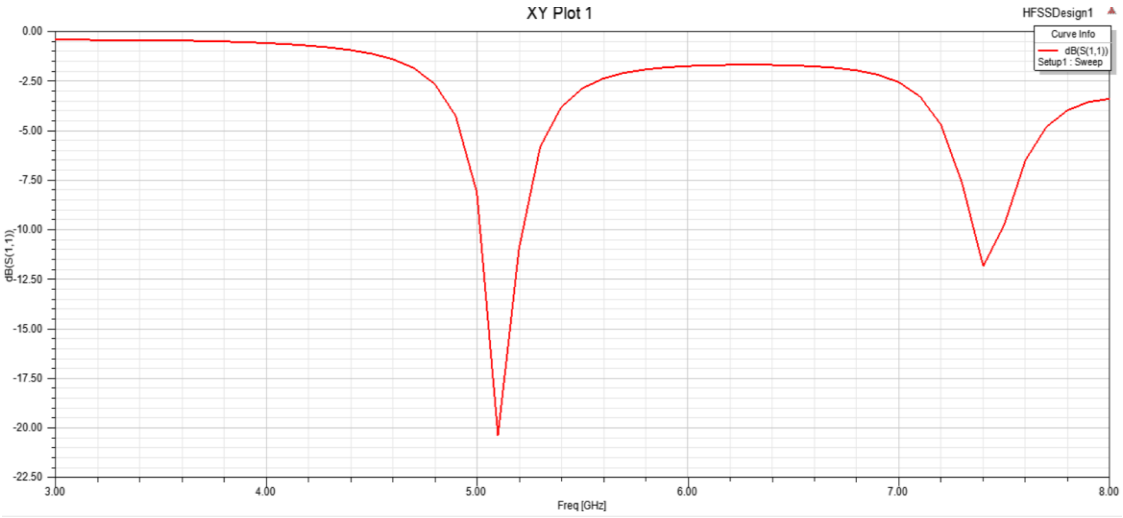

Figure 4.1.3 Return loss plot of the antenna

From the results, it is clear that, this design is not a choice for the required application since the gain demonstrated by the design is very less.

With a view to increase the gain of the antenna, a director was added to the above design, which showed an increase in the gain to 5.34 dB. The overall size of the antenna increased for a very little increase in gain, which made it not a wise choice for the application. The dimension of the director was 10mm in length and width was same as the patch antenna. The coupling capacitive gap between the patch and director was about 1mm. The design view from HFSS is given in Figure 4.1.4

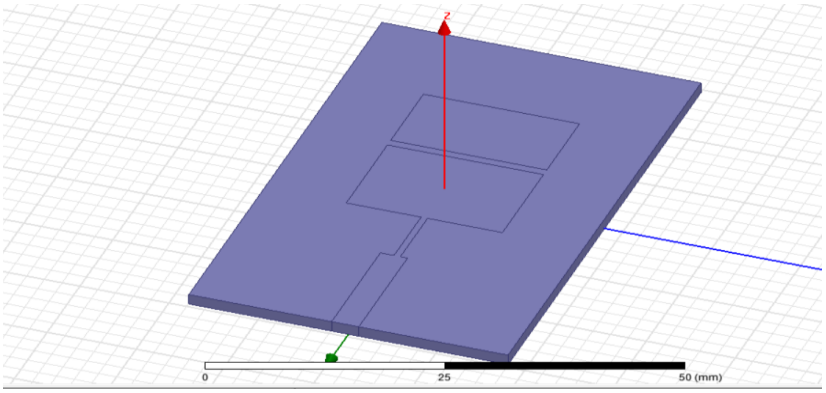

Figure 4.1.4 Patch antenna with director

Next, a patch antenna with an inset feed was tried, here the inset position is adjusted to match the impedance of the antenna to the feed line impedance. This antenna was found to be a promising candidate, showing a better gain of 7dB with a compact size and stable broadband radiation pattern. The following section gives the brief overview of the design results in HFSS along with fine tuning of design variables by parametric analysis to get the best possible radiation outcome.

The design starts with selecting the frequency of operation, to be around 5.6GHz. The permittivity of the dielectric substrate chosen was ε_r= 2.2 with height of 1.6mm. The length and width from the design equation was found to 16mm and 15mm respectively. The inset length was fixed to be quarter of the length of the patch which is 4mm. The feed line width and length along with inset width are fine-tuned from the parametric analysis. The width of the feed line and width of the inset was simultaneously varied from 0.3mm to 0.9mm and 0.2mm to 1mm respectively with feed length constant at 14mm. The return loss graph in Figure 4.1.5 shows that the bandwidth for the variation is almost the same (around 190 MHz), hence the variation with better S11 value is chosen. The width of the feed line and inset width finalized based on better return loss value is found to be 0.5mm and 1mm respectively.

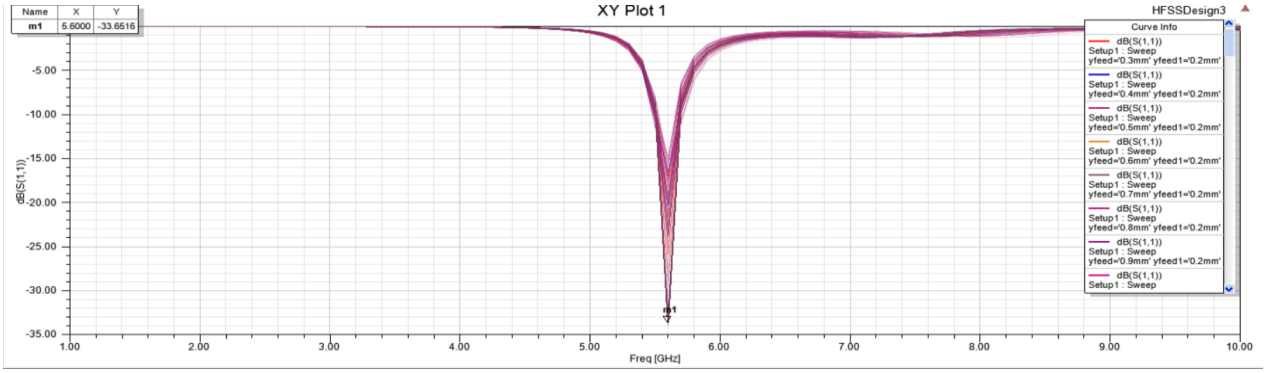

Figure 4.1.5 Parametric analysis on feed line width and inset width for an inset fed patch antenna

Now the length of the feed line is varied keeping the feed line width constant at 0.5mm and inset width at 1mm. The parametric analysis from HFSS is shown in Figure 4.1.6. The feed length after the analysis is fixed to be 15mm based on higher return loss value, since bandwidth for all variations is the same.

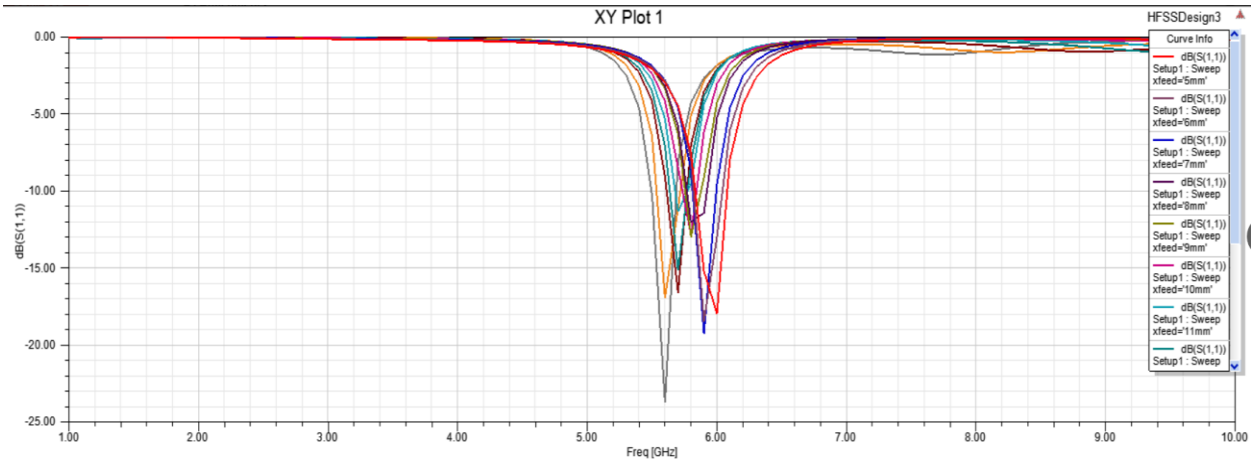

Figure 4.1.6 Parametric analysis on feed line length

The S11 graph of the optimized antenna, HFSS design layout, radiation pattern is shown in Figure 4.1.7, Figure 4.1.8 and Figure 4.1.9 respectively. The bandwidth of this antenna is around 190 MHz.

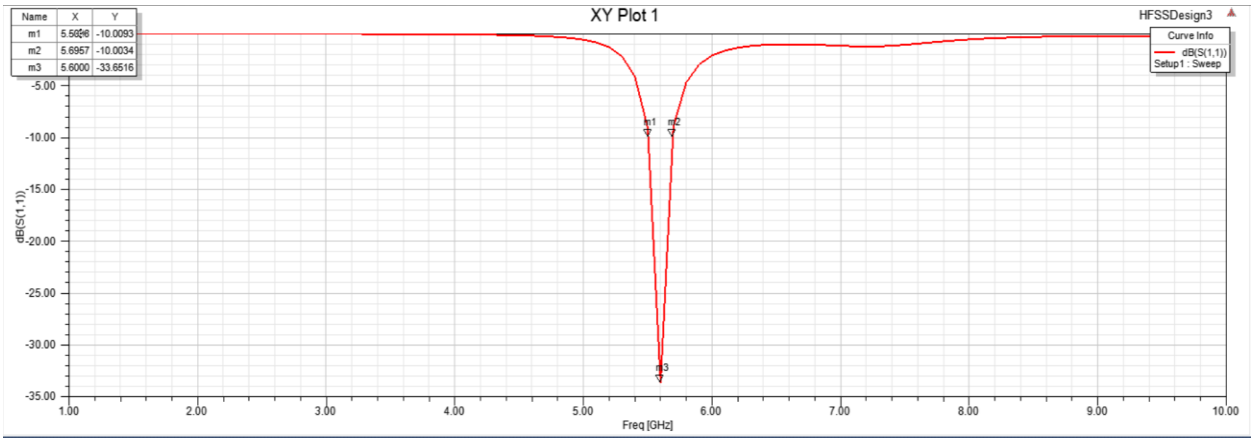

Figure 4.1.7 S11 of the optimized inset fed patch antenna

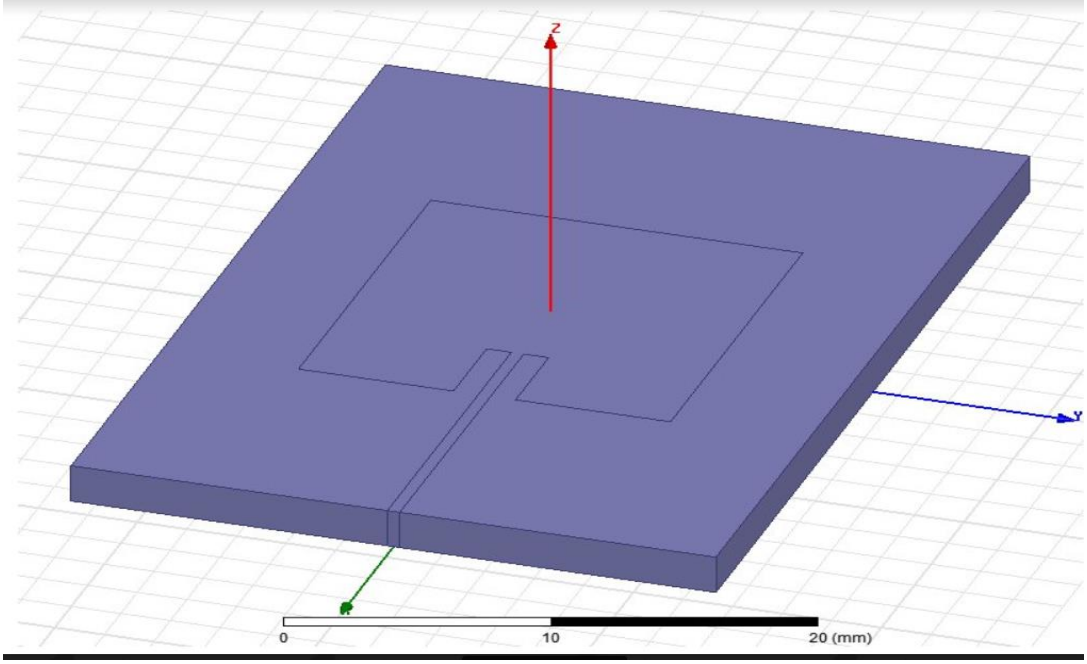

Figure 4.1.8 Inset fed patch antenna isometric view HFSS

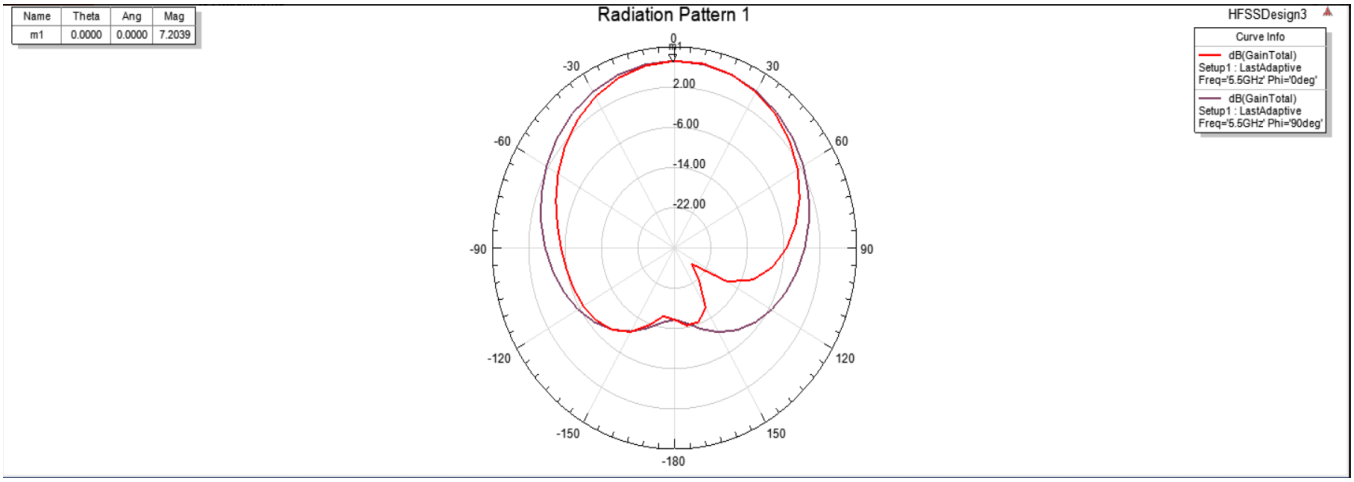

Figure 4.1.9 E (phi=0 deg, x-z plane) and H (phi=90 deg, y-z plane) plane radiation pattern of the optimized antenna

From Figure 4.1.9 the overall gain of the antenna is 7.2dB. This is a better and an optimum gain for a single antenna element, showing the required broadside radiation pattern and can prove to be an effective candidate for antenna array with minimal elements and maximum gain with a good beam steerability, since the E and H plane radiation pattern are almost wide

enough [3]. After this design, there was subsequent design modification performed to this basic patch, with a view to mainly increase on the gain slightly, as well as to bring about an increase in the bandwidth. The modifications done are to the geometry of an inset fed patch along the width, the radiating edge of the patch.

A sierpinski arrow head curve on an isosceles triangle with second iteration was done. Sierpinski triangles are usually drawn to create a multiband antenna, but such a design has less electric aperture, since conductive surfaces are cut, resulting in a low gain antenna. Here, instead of cutting the conducting surface, a curve is drawn with a view to increase on the gain of the antenna. Following the isosceles 2nd iteration sierpinski curve, a 3rd iteration equilateral sierpinski curve and a staircase structure protrusion along the width of the antenna were designed. All these radiating antennae had almost same gain or even a few tenths of a dB lesser gain to the original basic inset fed patch antenna. The bandwidth of operation remained the same. The design layout, radiation pattern as well as S11 of the above-mentioned designs are given from Figure 4.1.10 to Figure 4.1.18.

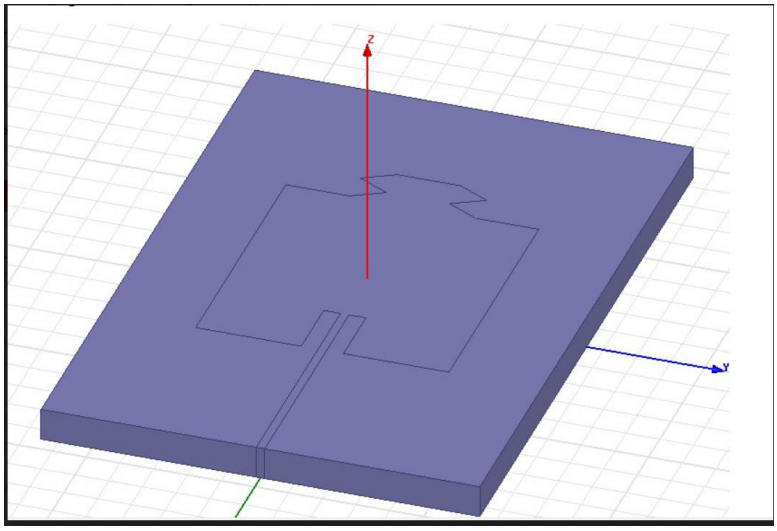

Figure 4.1.10 Sierpinski arrow head 2nd iteration from an isosceles triangle

Figure 4.1.10 depicts the 2nd iteration arrow head along the width of the radiating edge of the patch.

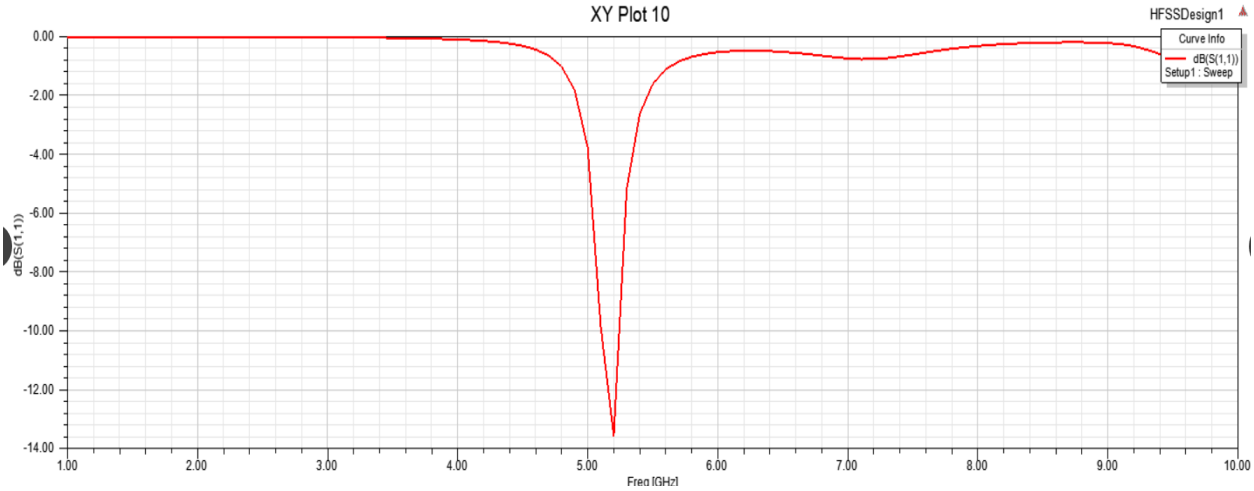

Figure 4.1.11 S11 of sierpinski 2nd iteration curve inset fed patch antenna

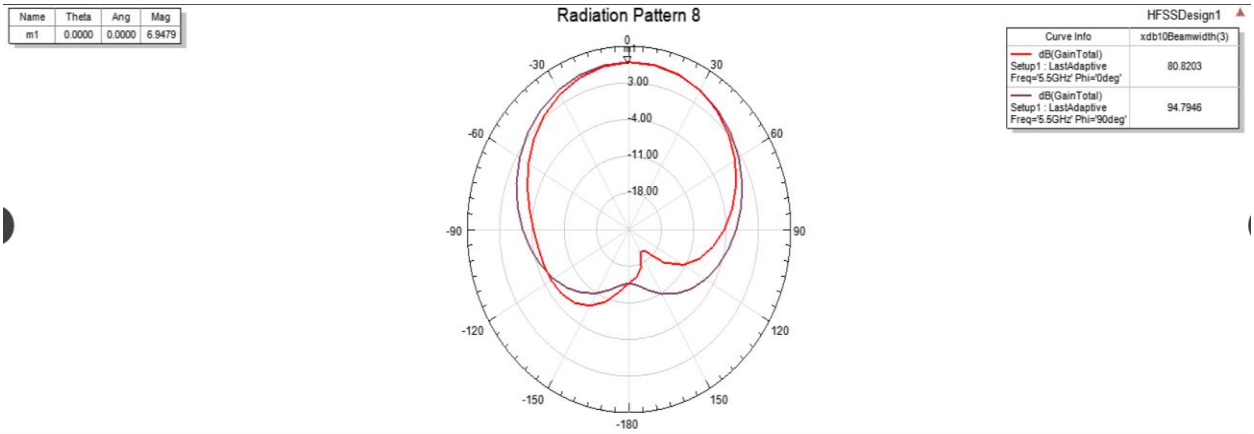

Figure 4.1.12 Radiation pattern of sierpinski 2nd iteration curve patch antenna

The gain of this antenna is lesser than the original microstrip inset fed antenna. The peak gain from Figure 4.1.12 is 6.9 dB.

The third iteration sierpinski arrow head curve using an equilateral triangle along one of the radiating edge of the antenna is shown in Figure 4.1.13. The overall gain of this antenna is found to be 7.04dB which is lesser than the patch antenna. The bandwidth is also not increased.

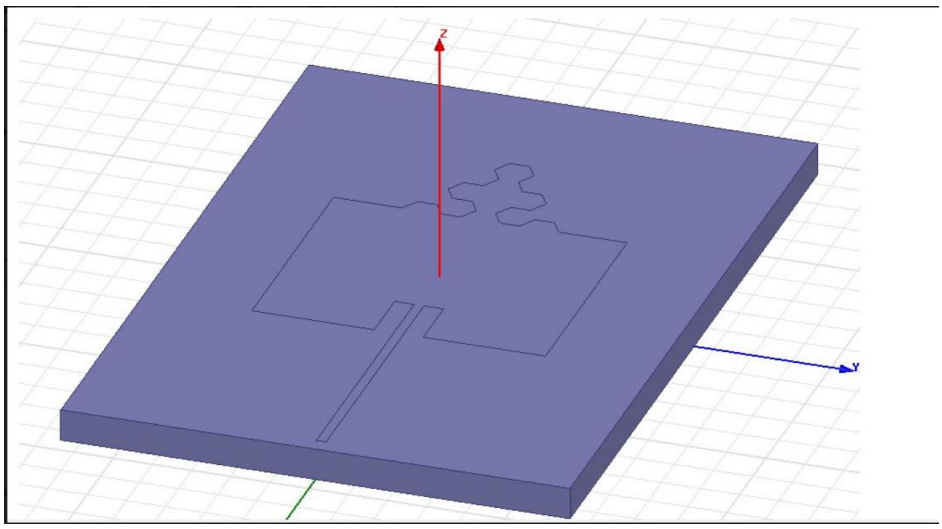

Figure 4.1.13 Sierpinski 3rd iteration arrow head curve patch antenna

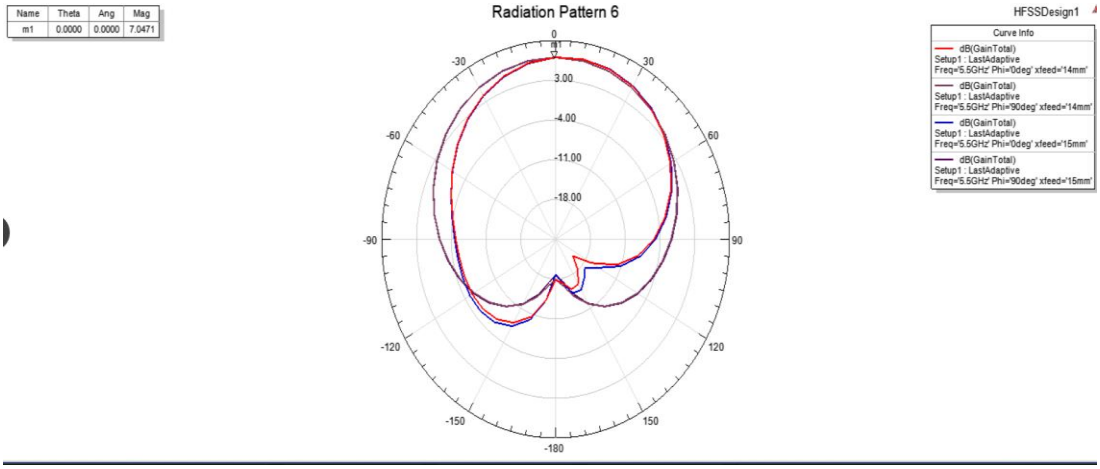

Figure 4.1.14 Radiation pattern of arrow head patch antenna

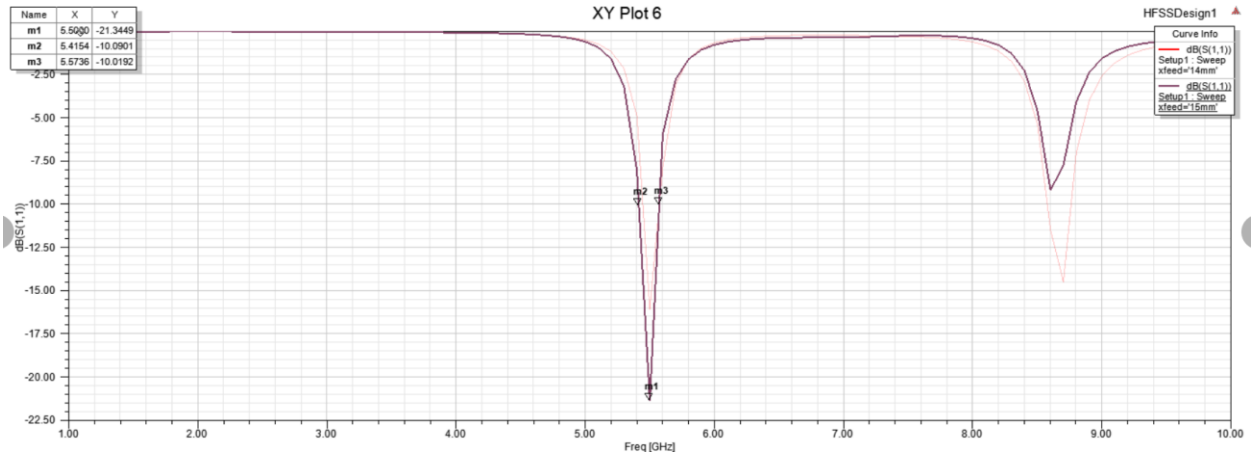

Figure 4.1.15 S11 arrow head patch antenna

The plots using HFSS for a staircase antenna is from Figure 4.1.16 to Figure 4.1.18

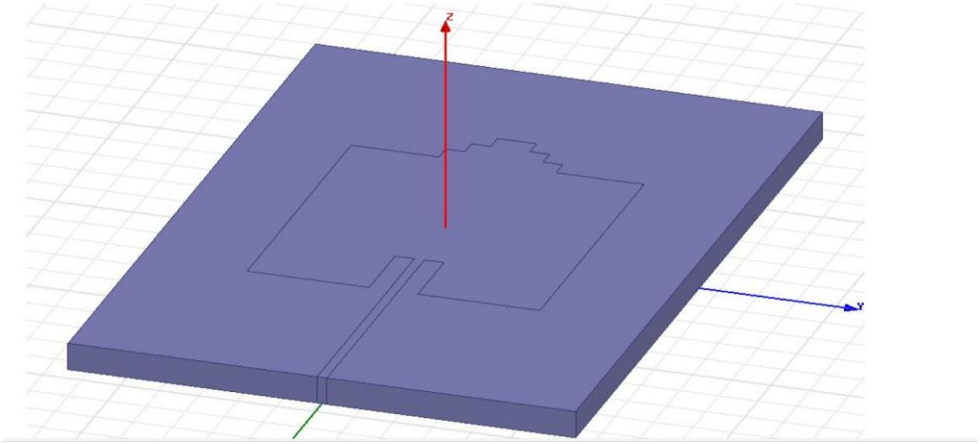

Figure 4.1.16 HFSS design layout of staircase antenna

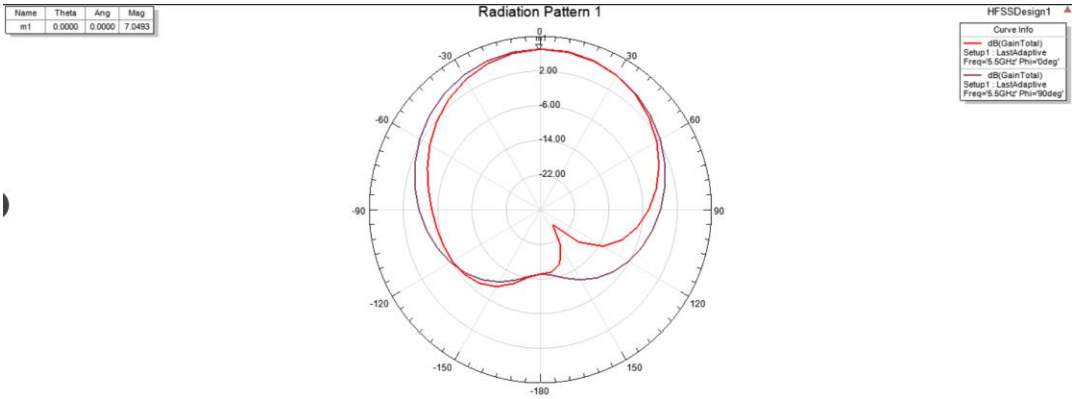

Figure 4.1.17 Radiation pattern of the staircase antenna

The radiation pattern shows that the overall gain is 7.04 dB.

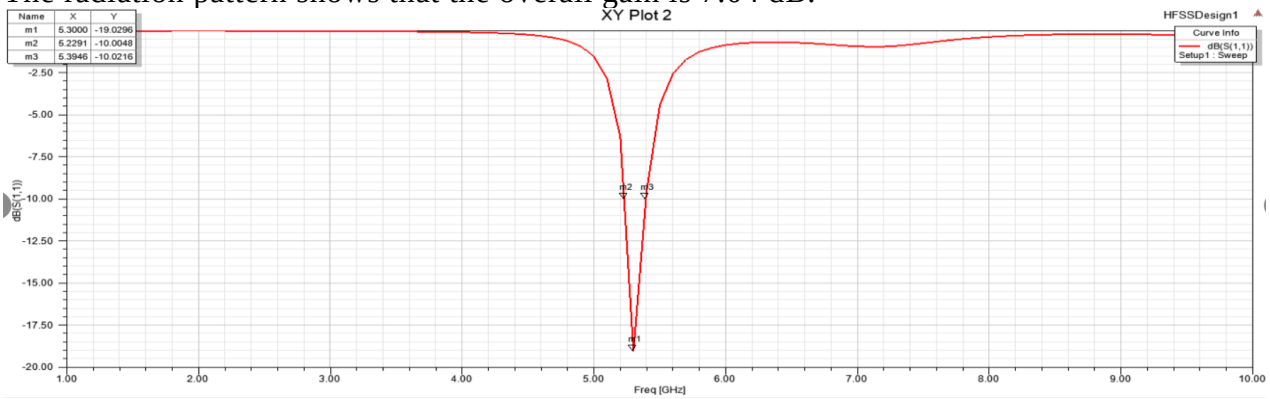

Figure 4.1.18 S11 of the staircase antenna

Apart from these designs, there were other designs carried out to increase the gain as well as bandwidth of operation. One such worth mentioning design is the modification of the ground plane with the use of metamaterials [10]. The same ground plane geometry as shown in [10] is replicated here.

The ground plane view is as shown in Figure 4.1.19.

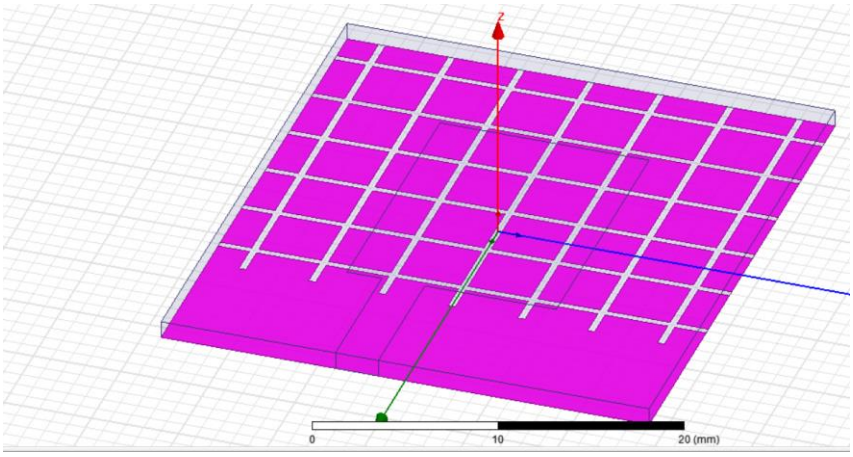

Figure 4.1.19 patch antenna with metamaterial ground plane

The radiation pattern is shown in Figure 4.1.20. The radiation characteristics is deviated from the broadside direction due to modified ground plane making it unsuitable to have a reference main beam direction in case of array formation. The overall gain is reduced to 5dB. The bandwidth as seen from S11 graph in Figure 4.1.21 is very high (2.1GHz) for this antenna. Since the gain and radiation characteristics are not adequate, it is considered unsuitable for the current application.

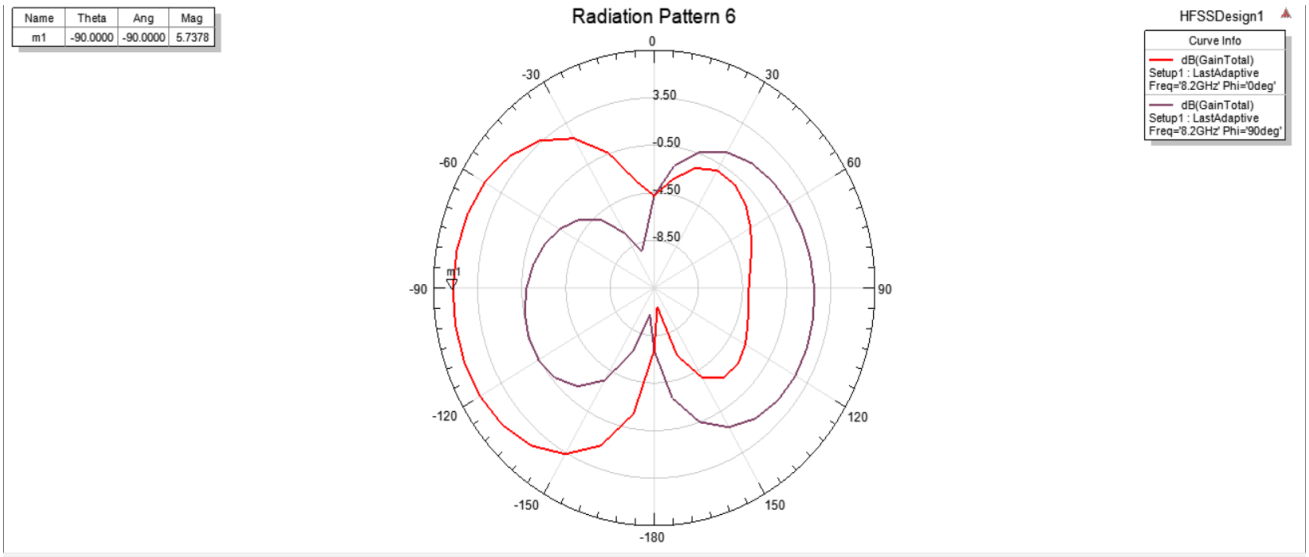

Figure 4.1.20 Radiation pattern of metamaterial ground plane patch antenna

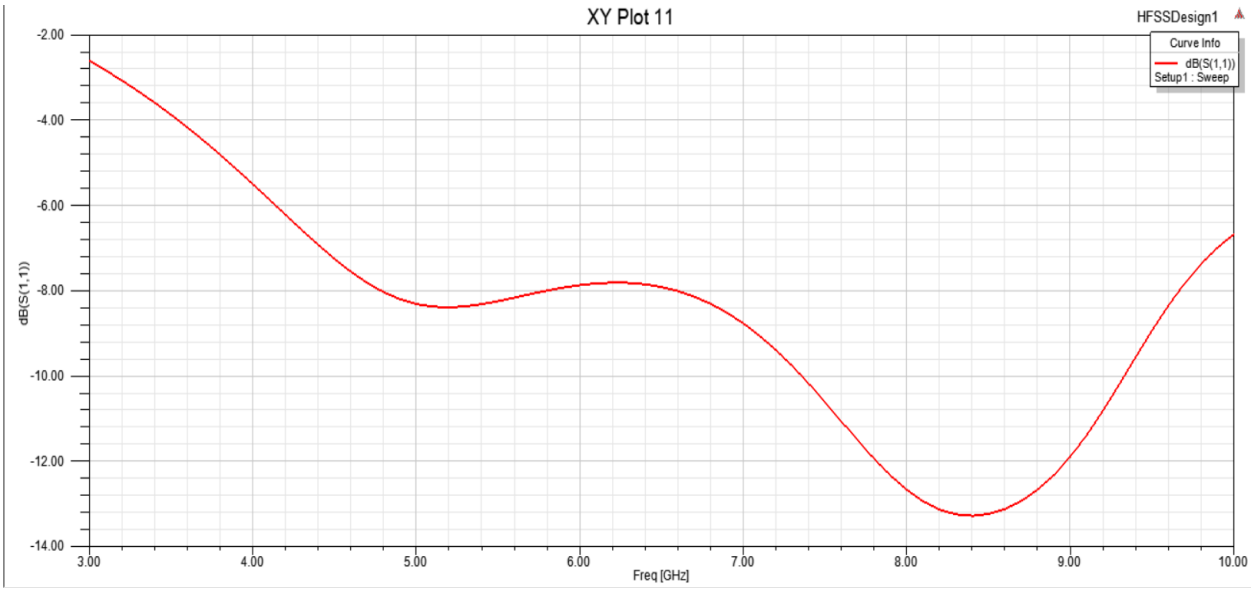

Figure 4.1.21 S11 of metamaterial ground plane patch antenna resonating at 8.2GHz

Another modified ground plane patch is presented which resonates at 5.6GHz, the gain is around 5.4dB. The radiation pattern is similar to the patch antenna in the E plane and omnidirectional in the H plane. This antenna is not considered suitable due to low gain and modified radiation pattern which requires many elements to scan in the H plane. The bandwidth of this patch is around 500MHz. Figure 4.1.22 shows the ground plane structure.

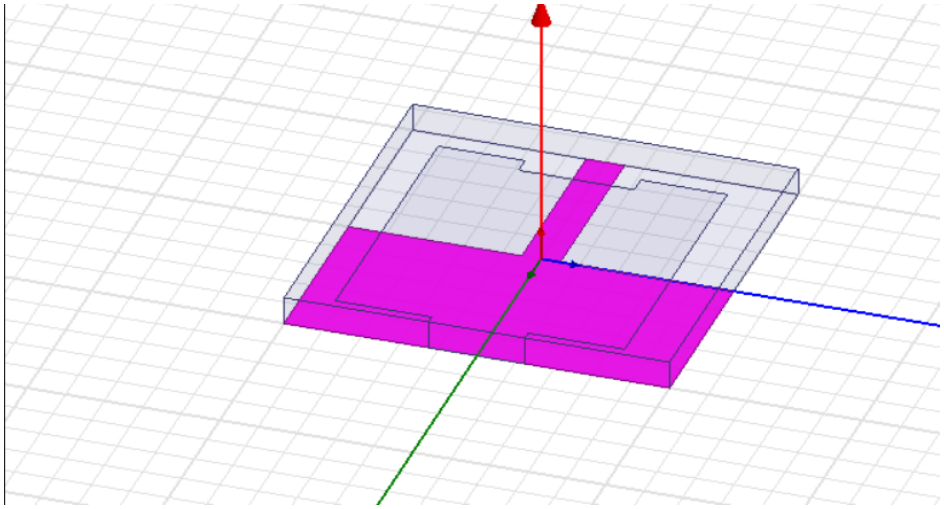

Figure 4.1.22 Antenna design with highlighted ground plane

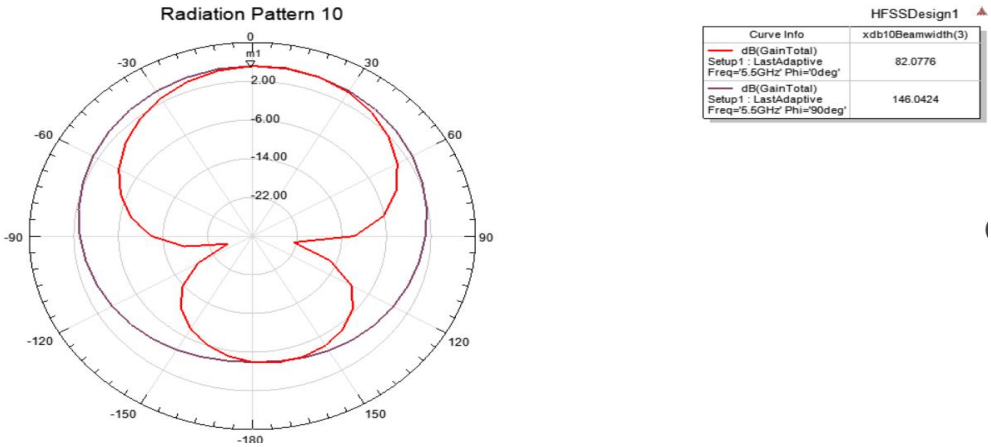

Figure 4.1.23 Radiation pattern of modified ground plane antenna

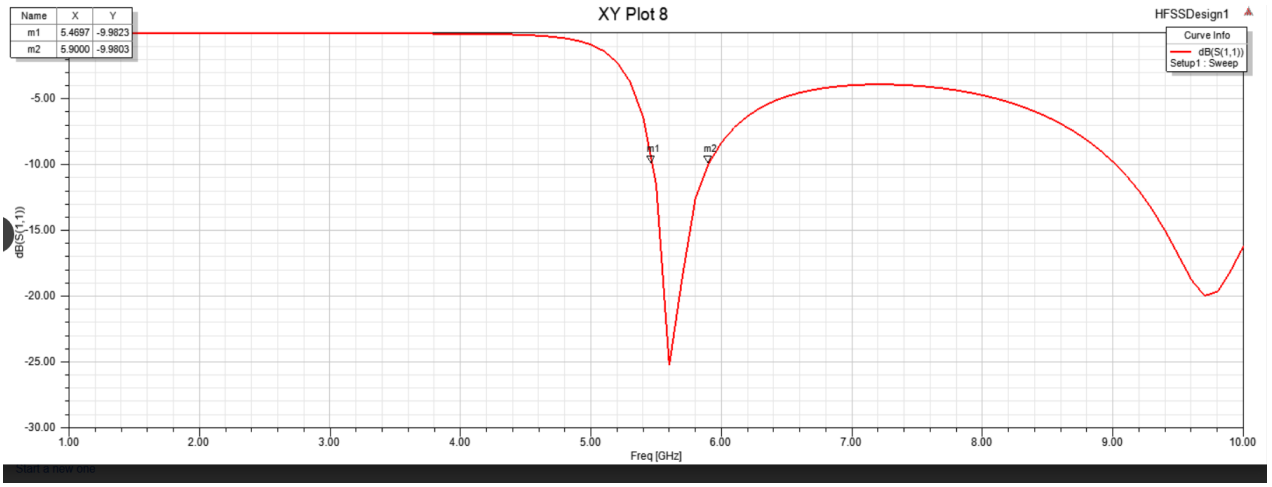

Figure 4.1.24 S11 of modified ground plane patch antenna

Also, several geometries of slots were cut on the basic inset fed patch, to obtain a wider bandwidth, but none of the design provided the required optimum characteristics with a good bandwidth. Hence, the tradeoff between the bandwidth and other design requirements (Gain, compact dimensions and simple reference radiation pattern), led to the choice of a basic inset fed patch antenna as the basic radiating element. It has the overall dimension of 16mm ×15mm × 1.6mm and a gain of 7.2 dB.

4.2 Antenna Array simulation in HFSS

The requirements for the antenna array design used in an unmanned aerial vehicle requires possible beam steering over the entire azimuth range. Hence, phased array antennas are designed using HFSS to steer the main beam to the maximum extent possible without deteriorating on the radiation pattern and gain falling below 10dB for an array.

First a corporate feed network [power divider network] array in both H and E plane were designed, using both 2 element and 4 element antennas to give a broadside radiation pattern. In order to steer the beam, phase shifters are required to be used. The phase shifting is achieved in HFSS by individually feeding each element of the array with separate lumped ports with appropriate phase shift between them, to steer the beam to the required direction. The gain obtained in broadside direction when a corporate feed network has been used is slightly lesser than the gain obtained by individually feeding antenna elements. Hence, there is not much difference between the losses incorporated in a network to that of individually fed elements.

The linear array design consisting of 2 and 4 elements were carried out in both E and H plane. The gain of 2 element array is less than 10dB and hence 4 element array was considered. The overall dimension of the linear E plane 4 element array with center spacing between elements, slightly larger than λ/4, that is for separation distance of 26mm, is 4.16cm ×10.4cm×0.16cm. The overall dimension of the array in H plane is given by 4.16cm ×9.8cm×0.16cm. The center to center distance in H plane is 24mm. To achieve the same gain of 12.2dB in E plane the center to center distance between 2 elements is 2mm larger than that of H plane. The figure 4.2.1 and 4.2.2 shows the E plane array and radiation pattern of the array respectively. Figure 4.2.4 and Figure 4.2.5 shows the H plane array and radiation pattern respectively. The design is carried out in HFSS by individually feeding the ports based on the requirements to apply the appropriate phase shift to direct the main beam in the required direction.

In a H plane array, non- radiating edges are spaced adjacent to each other and E plane array has radiating edges adjacent to each other.

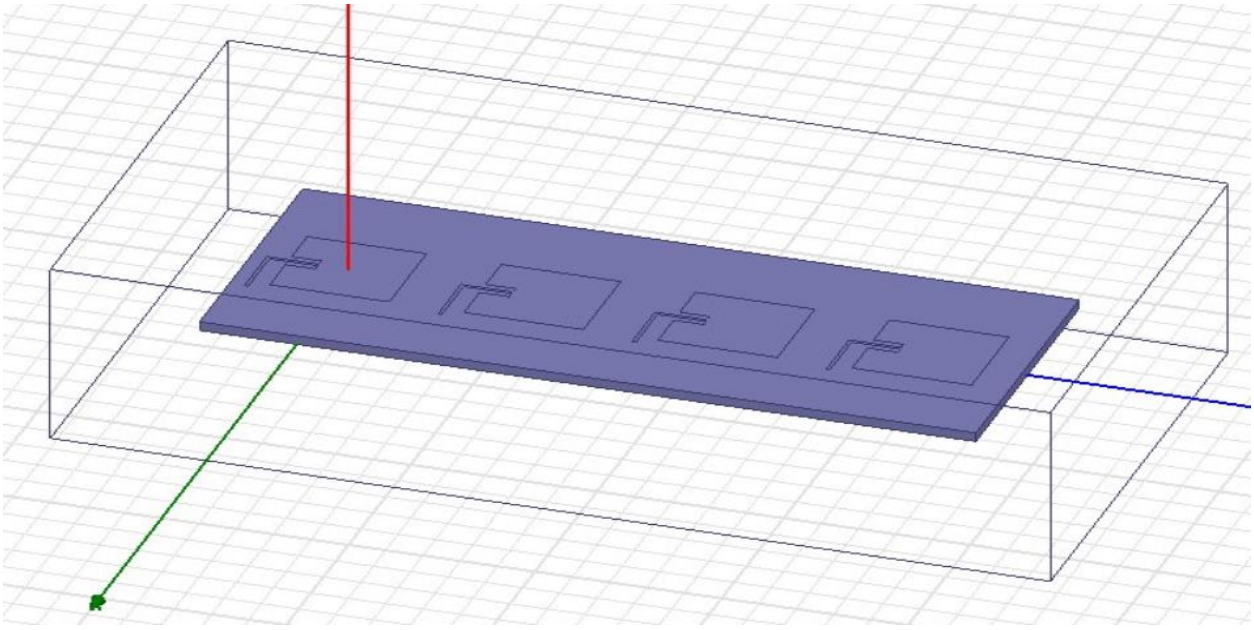

Figure 4.2.1 E plane patch antenna array with 4 elements

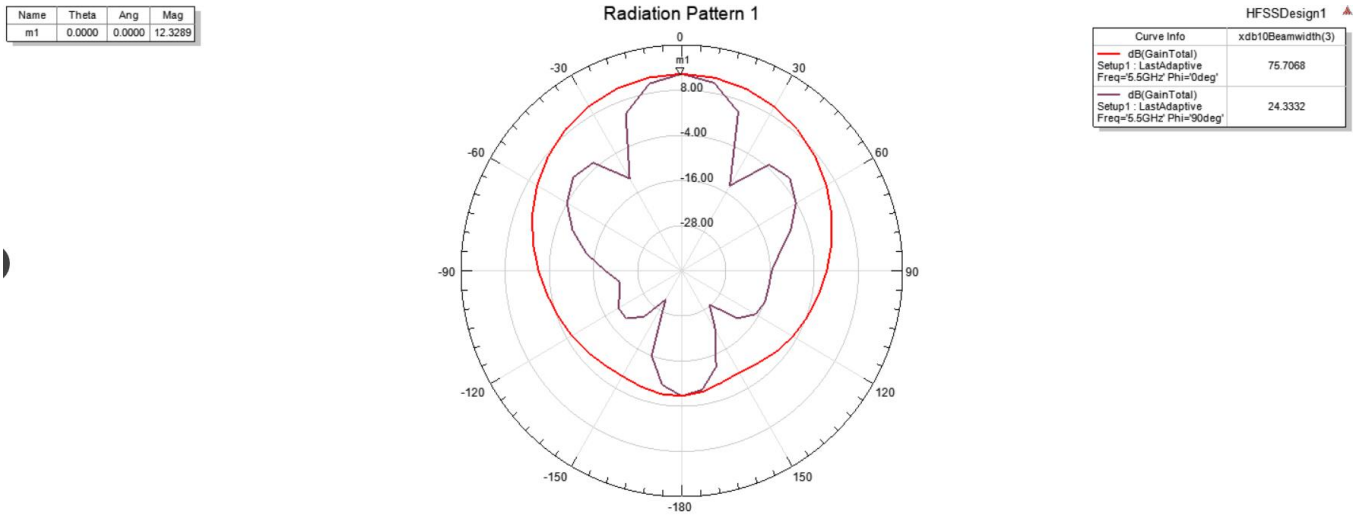

Figure 4.2.2 E plane array radiation pattern

Here in Figure 4.2.2, since elements are placed in E plane. Therefore, E plane of the antenna, that is the y-z plane has a directional beam whereas H plane that is the x-z plane has an omnidirectional beam. The longer feed length of the inset feed (as seen in Figure 4.2.1) in case of the E plane array is determined by parametric analysis from 5mm to 12mm in steps of 1mm, while keeping the shorter length constant at 7mm. The optimum longer inset feed length is found to 9mm from the graph shown in Figure 4.2.3.

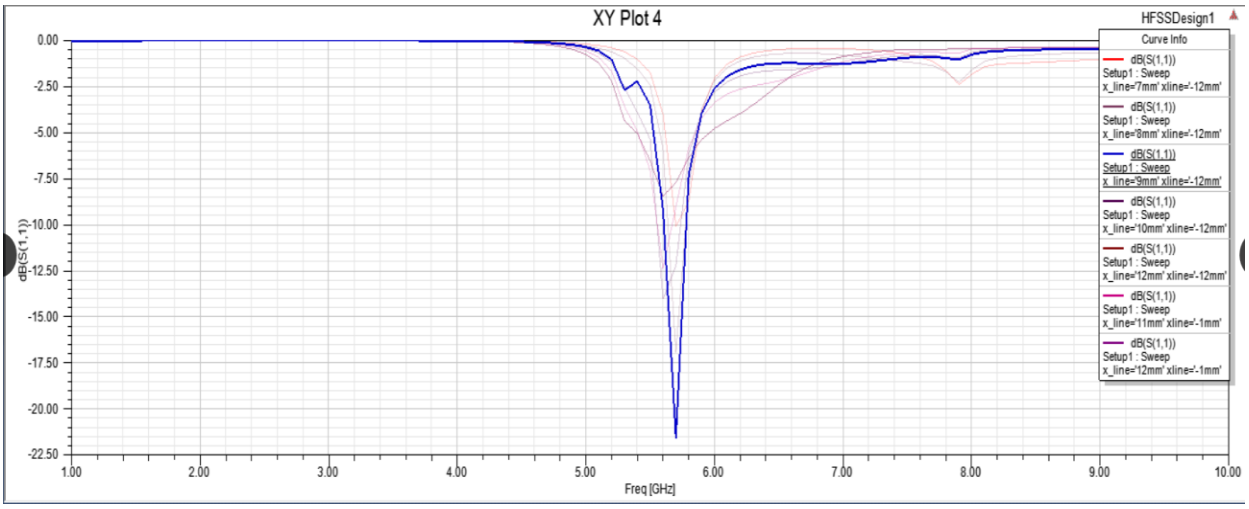

Figure 4.2.3 S11 plot showing the parametric analysis for E plane array.

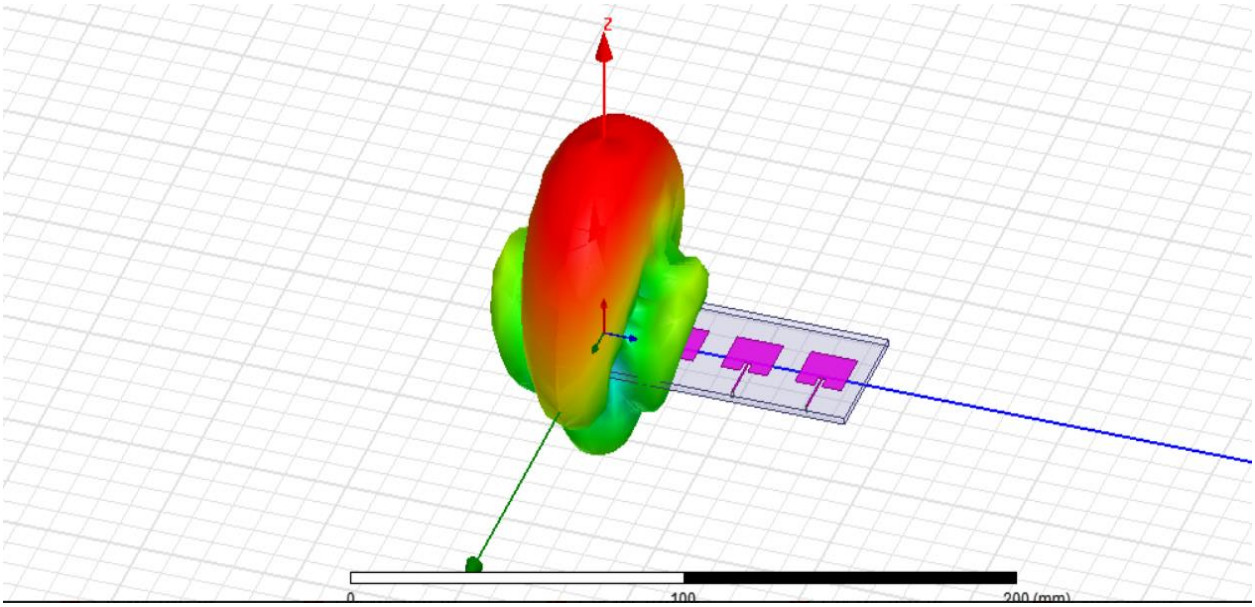

Figure 4.2.4 H plane array with 3D polar radiation pattern

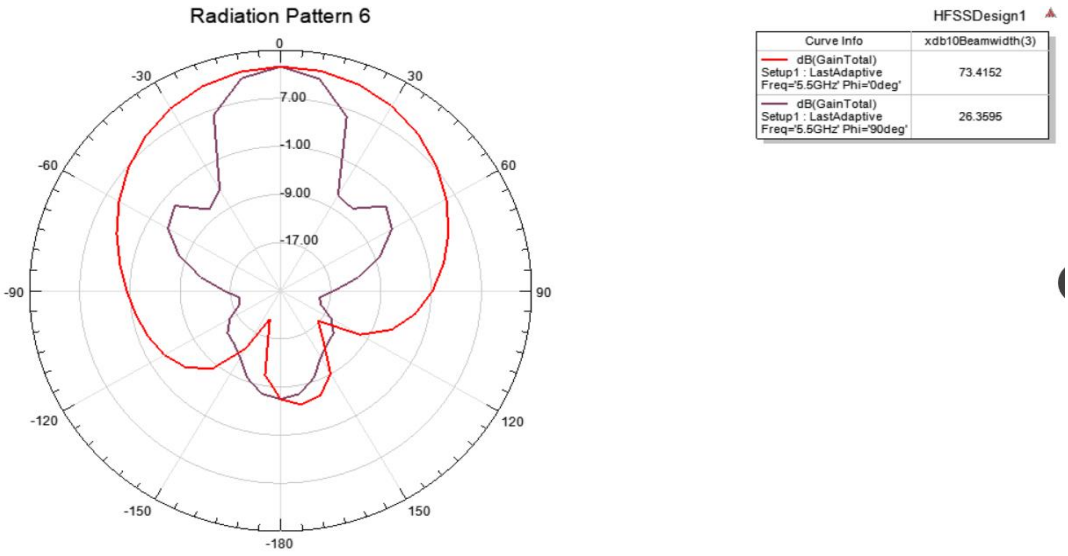

Figure 4.2.5 H plane array radiation pattern

Here in Figure 4.2.5, since elements are placed in H plane. Therefore, H plane of the antenna, that is the y-z plane has a directional beam whereas E plane that is the x-z plane has an omnidirectional beam.

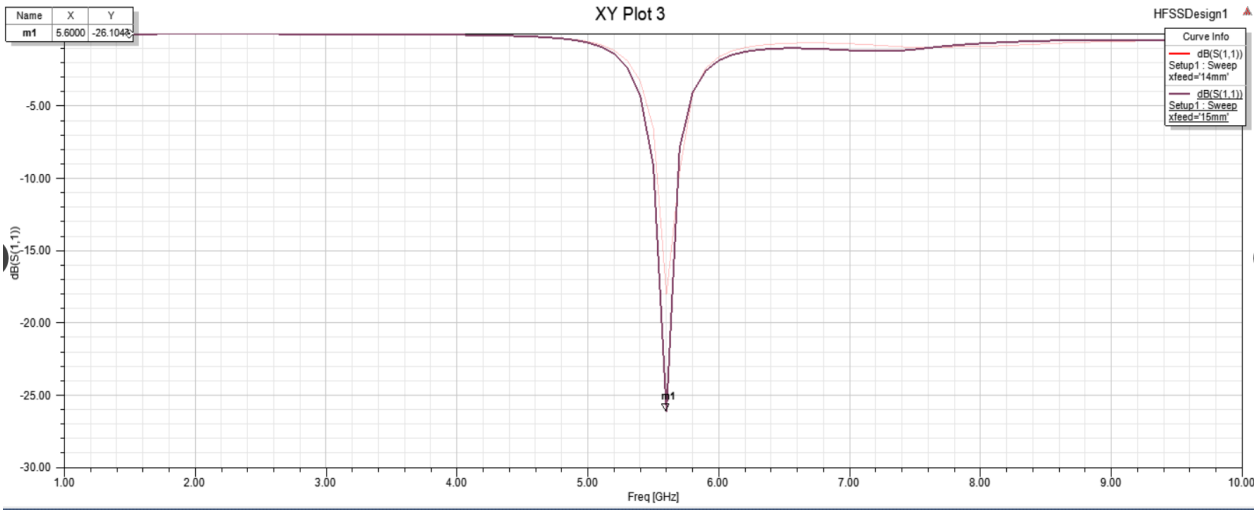

Figure 4.2.6 S11 of H plane array

Since the half power beam width as seen from the pattern is around 26 degrees, the phase shifts are done in a scan range of 10 degrees so that there no blind spots observed, which can result in loss of a communication link. Both H and E plane linear array are capable of scanning at range of ±40° from the broadside direction which is considered as the reference. Figure 4.2.7 to Figure 4.2.10 illustrates the scanning range plots with 10 degrees shifts.

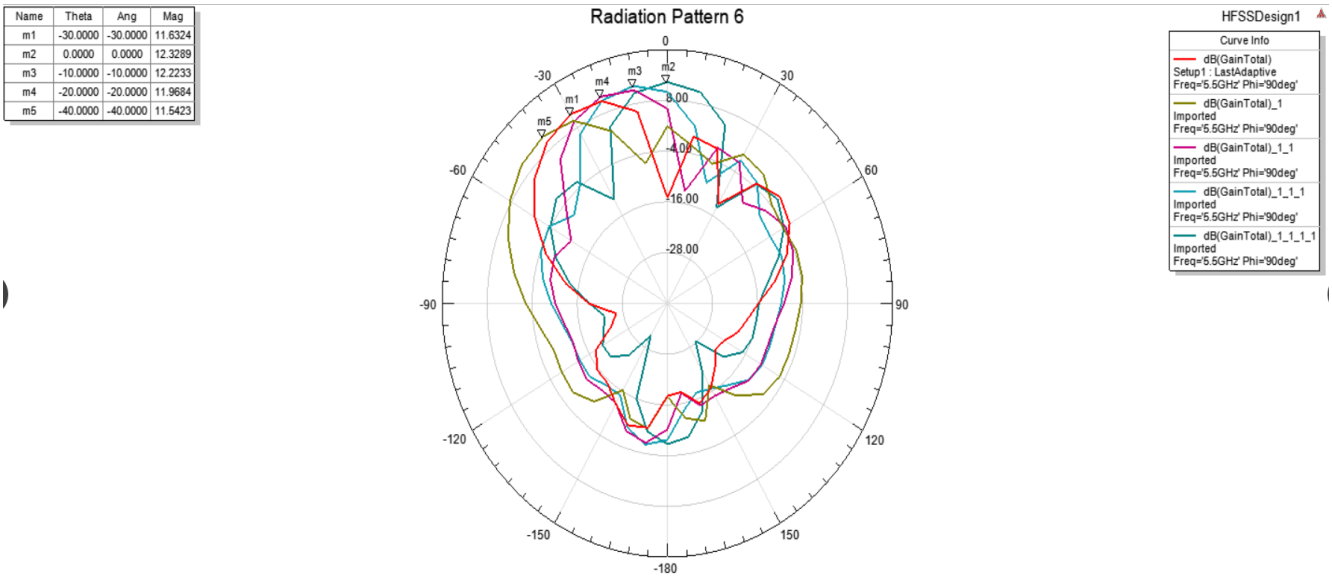

Figure 4.2.7 E plane array showing scanning from broadside direction to -40 degrees in steps of 10-degree phase shift

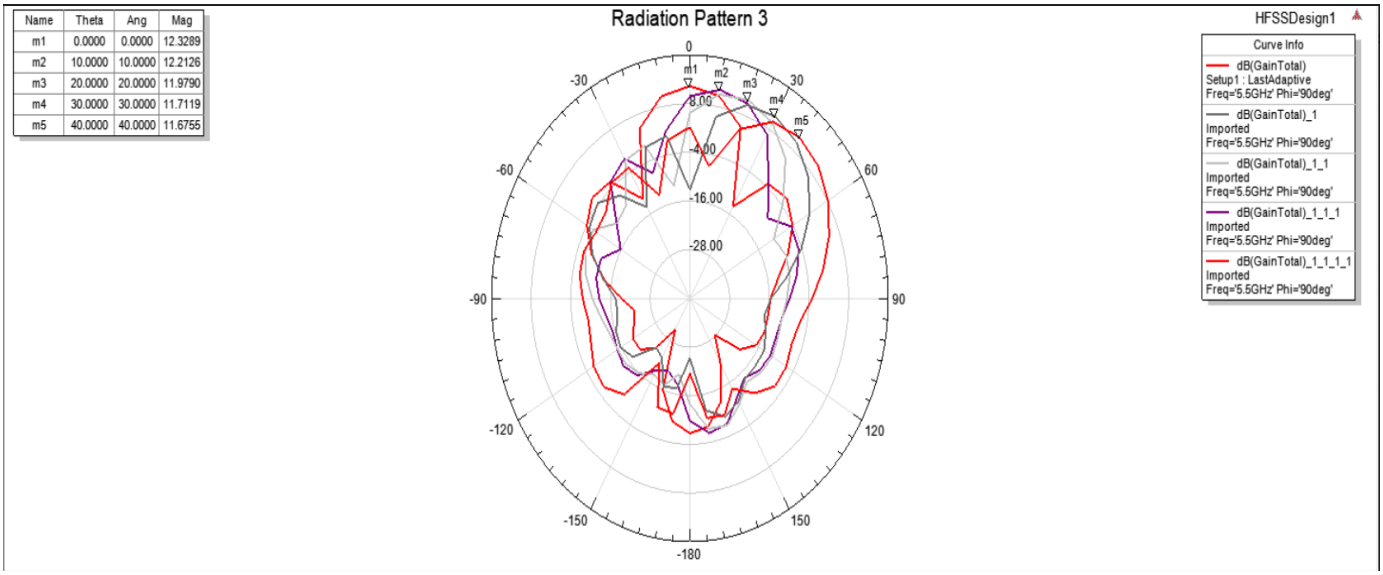

Figure 4.2.8 E plane array showing scanning from broadside direction to +40 degrees in steps of 10-degree phase shift

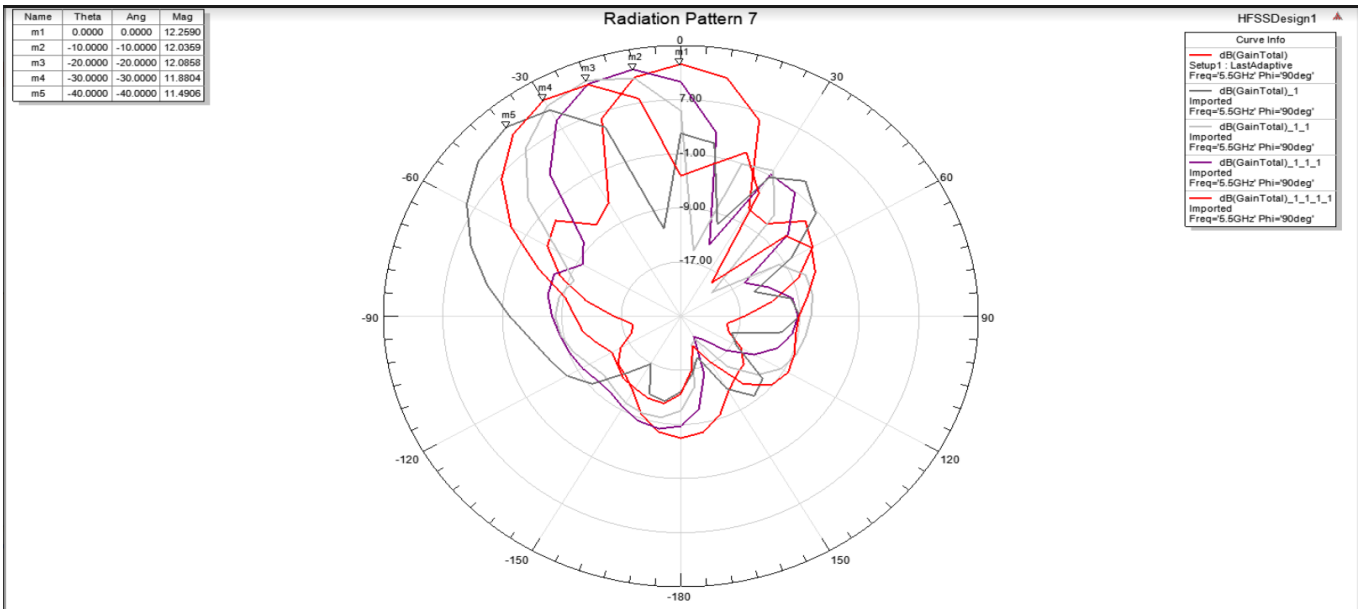

Figure 4.2.9 H plane array showing scanning from broadside direction to -40 degrees in steps of 10 degrees phase shift

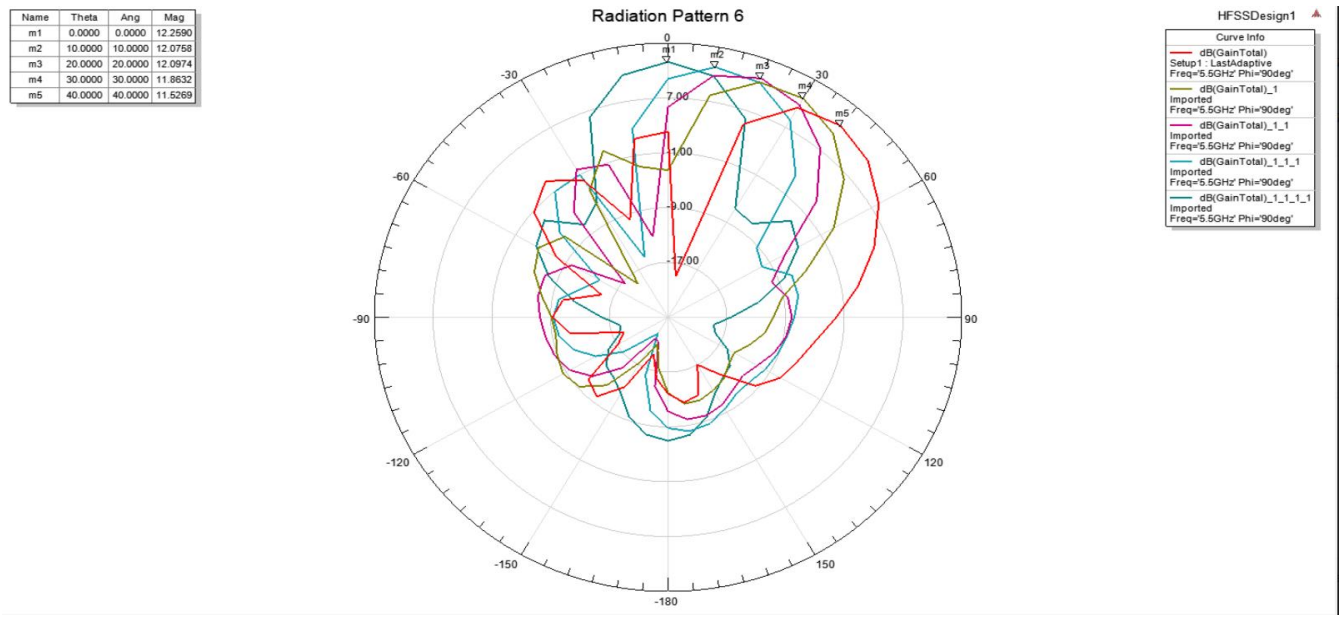

Figure 4.2.10 H plane array showing scanning from broadside direction to +40 degrees in steps of 10 degrees phase shift

The mutual coupling in an array environment is studied with the help of radiation pattern for a single element patch by comparing its gain when simulated in an isolated condition to that when placed in an array system. Figure 4.2.11 and Figure 4.2.12 show the radiation pattern of the 3rd element in E and H plane array when all the other three elements are terminated in a matched load. The variation is very minimal from a single element patch gain and radiation characteristics when compared with placement in an array. One can also observe a slight difference in pattern when the element is placed in E plane array and when placed in H plane array. The antenna element in H plane array show minimal deviation. Even, from the H plane array already discussed, one can infer that the H plane array performs slightly better and it is smaller in dimension, because the inter-element spacing is lesser compared to E plane array, for obtaining the same peak gain. The side lobe levels in H plane array is also less.

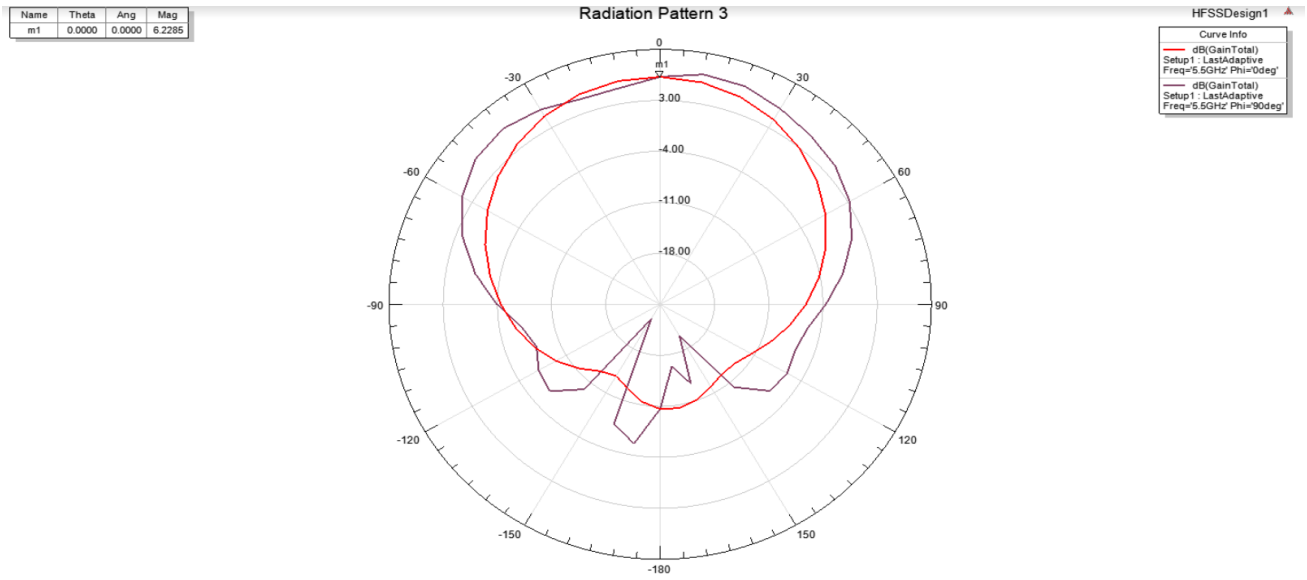

Figure 4.2.11. radiation pattern of the third element when placed in an E plane array

It can be noted from Figure 4.2.11 that there is around one dB decrease in the gain compared to individual isolated antenna element.

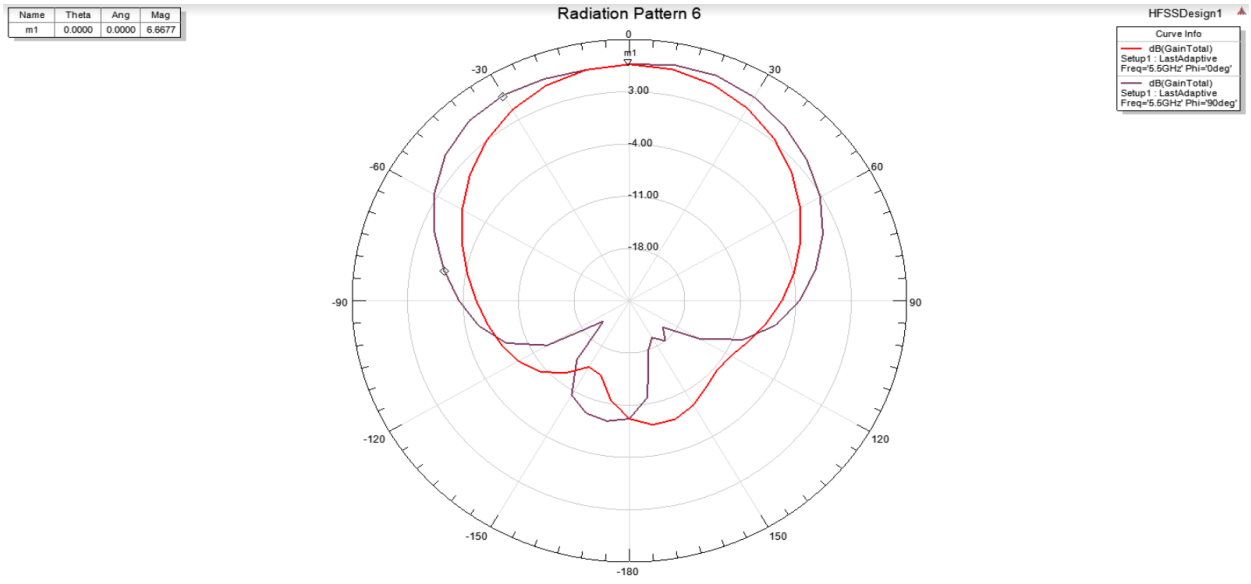

Figure 4.2.12 Radiation pattern of the third element when placed in an H plane array

From figure 4.2.12 antenna element gain in H plane array is about 0.6dB lesser than the standalone antenna gain.

A single array can have the beam scanning range of ±40 from the broadside direction. Hence it covers a total scan range of 90 degrees. To cover the complete azimuth range four such arrays ($4*90= 360^0$), are required to be present in a square arrangement in which only one array is active at a particular instance of time. This array which is active scans over 90 degrees in the azimuth plane (here theta=90 plane or x-y plane, for patch array oriented in y-z plane), after which, the 90^0- rotated array with respect to the previous array takes over to scan the rest of the azimuth plane. A system with such design can scan over the entire azimuth range.

The CAD model of such a system as well as illustration on the radiation pattern in polar form, when such switching between array takes place is discussed here, through series of HFSS results. The system individually consisting of both H plane array and E plane array are depicted in Figures 4.2.13 and 4.2.14 respectively. It is observed that, when obtaining the polar plot to depict the scanning capability, only one array was fed in the presence of the other three arrays, while the rest was terminated in a matched load, the radiation plot showed no influence by the presence of other arrays unlike the case of a single antenna element which shows the deviation. Figures from 4.2.15 to Figure 4.2.18 depicts the azimuth scanning polar plots for E and H plane array operating individually. From the results obtained it can be inferred that H plane array system is better than E plane array system, as the overall dimension for H plane array is slightly less with same radiation pattern and peak gain.

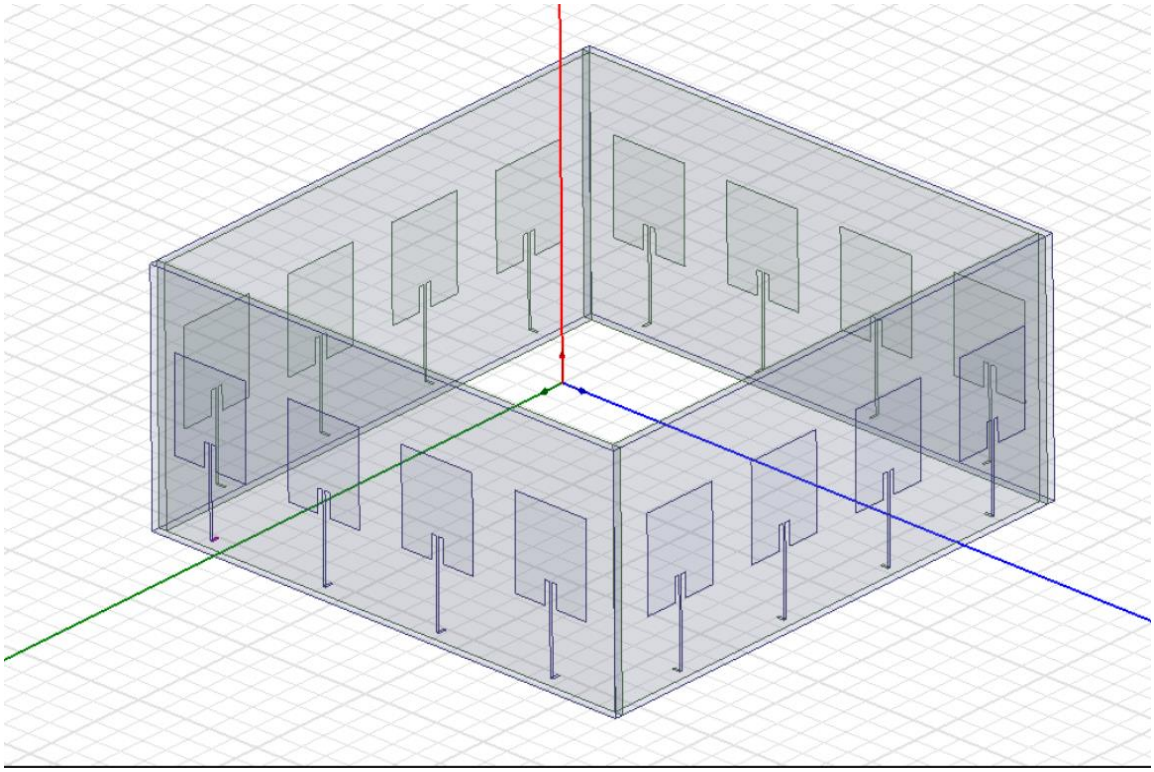

Figure 4.2.13 H plane 4 array system

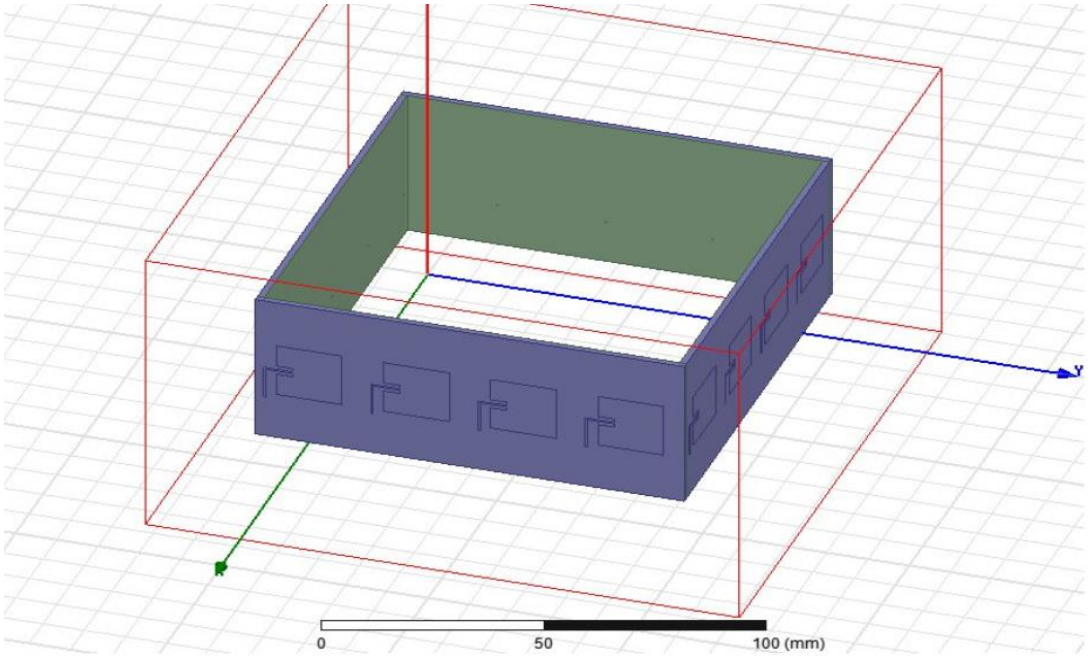

Figure 4.2.14 E plane 4 array system

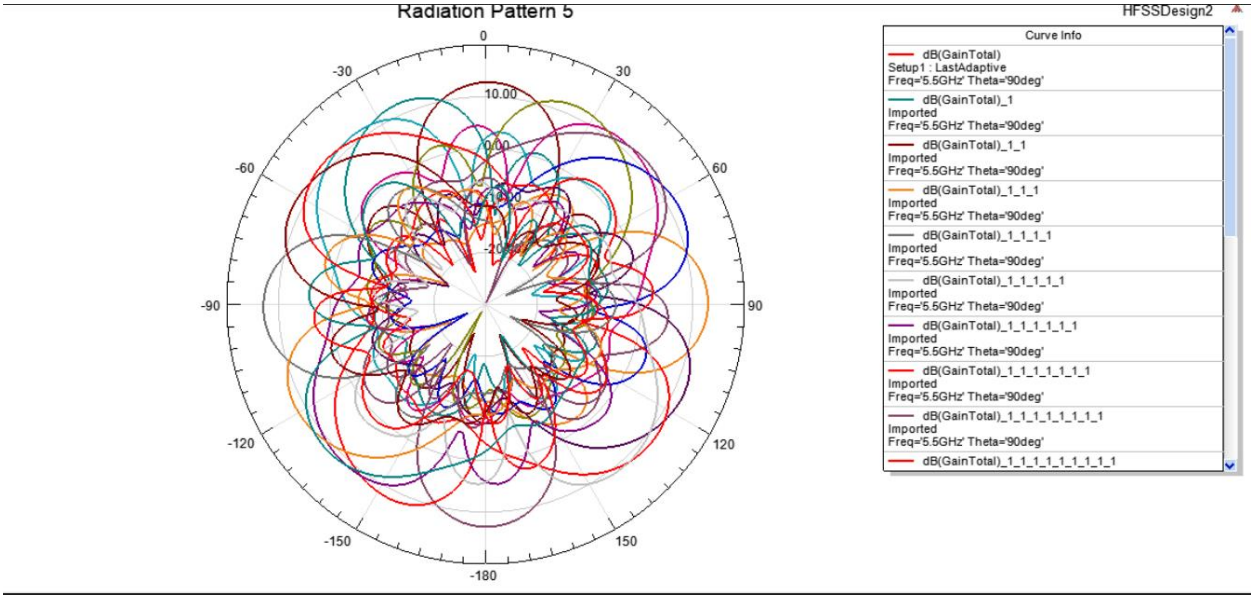

Figure 4.2.15 H plane 4 array system showing entire scanning over the azimuth by switching between arrays. Each array shows broadside beam as well as steered $\pm 30^0$ and $\pm 40^0$ beams

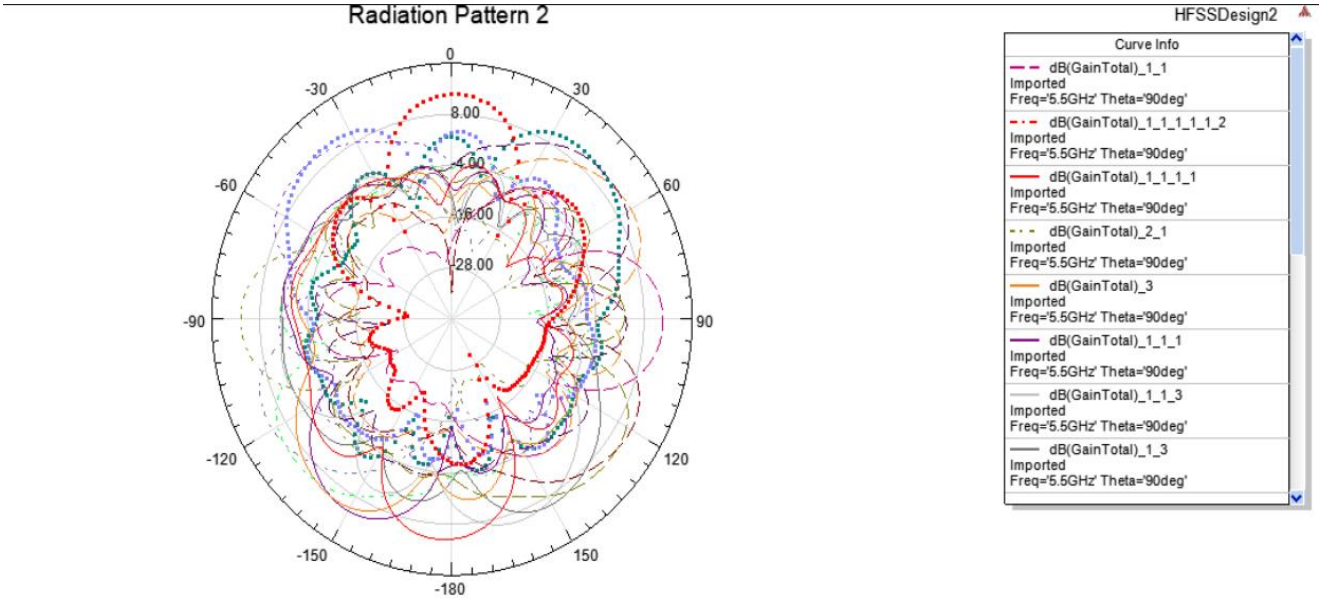

Figure 4.2.16 E plane 4 array system showing entire scanning over the azimuth by switching between arrays. Each array shows broadside beam as well as steered $\pm 30^0$ and $\pm 40^0$ beams

Name	Phi	Ang	Mag
m1	0.0000	0.0000	12.7738
m2	-90.0000	-90.0000	12.9223
m3	180.0000	180.0000	12.8308
m4	90.0000	90.0000	12.9519

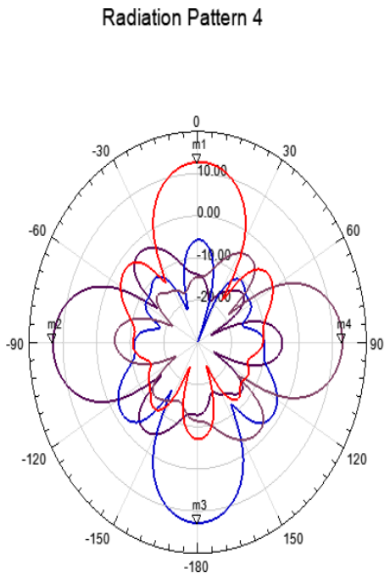

Figure 4.2.17 H plane 4 array system showing only the broadside beams of each switched array

Name	Phi	Ang	Mag
m1	0.0000	0.0000	12.7715
m2	90.0000	90.0000	12.7731
m3	180.0000	180.0000	11.5479
m4	-90.0000	-90.0000	12.7483

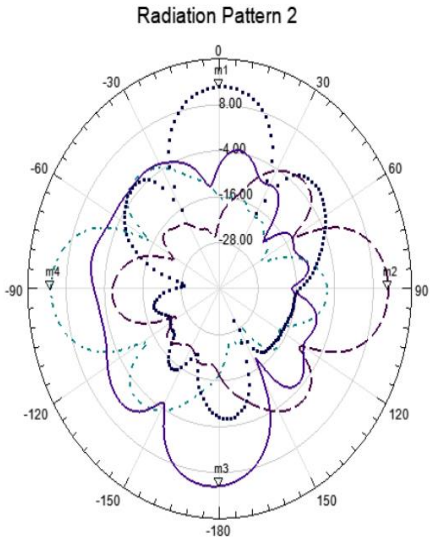

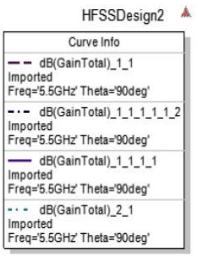

Figure 4.2.18 E plane 4 array system showing only the broadside beams of each switched array

When the scanning is required in both principle planes simultaneously, then a planar array system must be designed which is capable of scanning in both dimensions.

4.3 Antenna Fabrication

A single element patch antenna was fabricated and tested for return loss and radiation characteristics. The antenna was fabricated on RT duroid dielectric substrate with a thickness of 1.4mm. The fabrication was done using the milling machine from bantam tools, present in UTA Markers Space. The single element inset fed patch antenna with the dimensions mentioned earlier took about 30 minutes to mill. The testing and analysis of the antenna for return loss and peak gain was carried out using Agilent handheld N9923A 6 GHz Vector Network Analyzer. The antenna fabricated is shown in Figure 4.3.1.

After the appropriate calibration of the equipment, the antenna showed two resonances, one at 4.7GHz and another at 6GHz. The resonance at 4.7GHz can be attributed to scattering from the substrate as well as the ground plane dimensions of the antenna is not accurate, and a larger ground plane would help to rectify this problem.

The milled antenna dimensions are slightly different from the actual HFSS simulation. The resonance at 6GHz is because of the shorter dimensions of the patch length after milling.

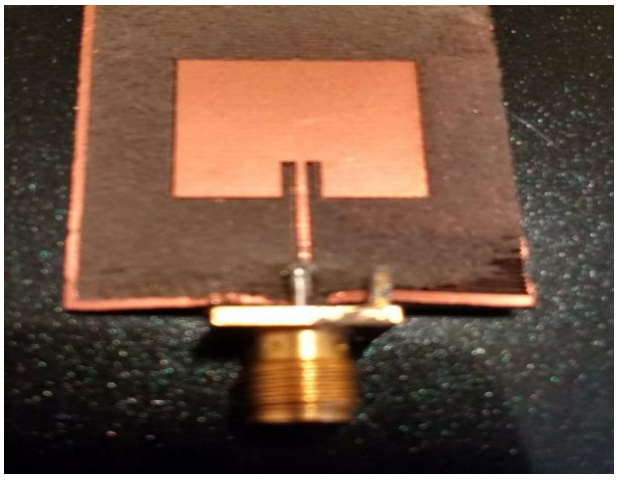

Figure 4.3.1 Milled single element inset fed patch antenna

The return loss values at 4.7 GHz is found to be 21.028dB and 6.21dB at 6GHz. The VSWR is 1.19 at 4.719GHz and 2.9 at 6GHz. From the Smith chart the matching at 4.7GHz is found to be 55.6 -j7.1 ohm and 35.1 -j 46.5 ohm. The peak gain was measurement using two horn antennas initially to measure the S21, and later one of the horn antenna was replaced by the inset fed patch antenna to obtain the S21. From these S21 measurements, gain at both the frequencies (4.7GHz and 6GHz) was calculated using Friis transmission equation. The cable loss at both the frequencies was also taken into consideration. The antennas are separated by a distance of 114 inches or 2.8956m. The obtained gain at 6GHz for the horn antenna is about 13dB. Using the horn antenna gain, the patch gain is calculated to be around 2dB. The poor gain of the patch antenna can be because of insufficient ground plane, not precise dimensions as simulated in HFSS is maintained after milling the antenna, hence the resonance of the antenna has shifted from 5.6GHz to 6GHz. Also, the SMA soldering is not done exactly at the center of the feed line. The patch shows negative gain at 4.7GHz.

Chapter 5

5.1 Summary

This thesis emphasizes on designing a suitable low profile, with simple geometry and standard broadside radiation pattern antenna element, which can be used in a phased array antenna system to provide the optimum scanning range with sufficient gain over the azimuth plane. A single array is not capable of covering the entire range of the azimuth, hence four antenna array system was used, to switch between them to cover the complete plane. The single antenna array is capable of scanning $\pm 40^0$ in the azimuth. The gain over the scanning range does not fall below 10 dB. The entire system occupies a planar surface (over which the array is mounted), of 10.4cm ×10.4cm when E plane array is used and 9.8cm × 9.8cm when H plane array is used.

5.2 Future Work

This thesis does not address the feeding network design to achieve the phase shift or the design of phase shifter units, either by analog design techniques or by digital beam formers. There is a requirement of individual port for each antenna element, which can give rise to various losses leading to degradation of the performance. This issue has not been talked about in this work. Again, electrical switches that are required to be used, its number as well as the pattern of operation has to be taken care of. Also, compact design with wider bandwidth and polarization diversity, so that there is no compromise on antenna misalignment which can results in failure of the communication link, are some of the important aspects that needs attention.

References

[1]. https://www.uavs.org/advantages

[2]. Gu, Yixin & Zhou, Mi & Fu, Shengli & Wan, Yan. (2015). Airborne WiFi networks through directional antennae: An experimental study. 2015 IEEE Wireless Communications and Networking Conference, WCNC 2015. 1314-1319. 10.1109/WCNC.2015.7127659.

[3]. C. M. Liu, S. Q. Xiao, H. L. Tu and Z. Ding, "Wide-Angle Scanning Low Profile Phased Array Antenna Based on a Novel Magnetic Dipole," in IEEE Transactions on Antennas and Propagation, vol. 65, no. 3, pp. 1151-1162, March 2017.
doi: 10.1109/TAP.2016.2647711

[4]. D. V. Navarro-Méndez, H. C. Moy-Li, L. F. Carrrera-Suárez, M. Ferrando-Bataller and M. Baquero-Escudero, "Antenna arrays for unmanned aerial vehicle," 2015 9th European Conference on Antennas and Propagation (EuCAP), Lisbon, 2015, pp. 1-5.

[5]. Kedar, Ashutosh & S Beenamole, K. (2011). Wide beam tapered slot antenna for wide angle scanning phased array antenna. Progress In Electromagnetics Research B. 27.. 10.2528/PIERB10100508.

[6]. Jing Nie, Yan-Qing Tan, Chun-Lin Ji and Ruo-Peng Liu, "Analysis of Ku-Band steerable metamaterials reflectarray with tunable varactor diodes," 2016 Progress in Electromagnetic Research Symposium (PIERS), Shanghai, 2016, pp. 709-713.
doi: 10.1109/PIERS.2016.7734429

[7]. S. E. Valavan, D. Tran, A. G. Yarovoy and A. G. Roederer, "Planar Dual-Band Wide-Scan Phased Array in X-Band," in IEEE Transactions on Antennas and Propagation, vol. 62, no. 10, pp. 5370-5375, Oct. 2014.
doi: 10.1109/TAP.2014.2343252

[8]. Constantine A. Balanis, Antenna Theory:Analysis and Design, 3rd edition, John Wiley & Sons, 2005, ISBN: 047166782X

[9]. Antenna-Theory.com Link: http://www.antenna-theory.com/

[10]. Li, Xueshi & Xu, Kaida & Zhou, Dong-Yue & Du, Fei & Liu, Zhi-Min. (2015). METAMATERIAL Extends Patch Antenna Bandwidth. Microwaves and Rf. 54. 58-64. http://www.mwrf.com/passive-components/metamaterial-extends-patch-antenna-bandwidth

[11]. Planar arrays Link: http://nptel.ac.in/courses/108101092/

[12]. https://www.dji.com

[13]. http://www.ansys.com/Products/Electronics

[14]. J. M. Inclán Alonso and M. S. Pérez, "Phased Array for UAV Communications at 5.5 GHz," in IEEE Antennas and Wireless Propagation Letters, vol. 14, pp. 771-774, 2015. doi: 10.1109/LAWP.2014.2379442

[15]. S. Livingston, G. Shows, J. J. Lee, B. Chiou and K. A. Hunten, "A structurally integrated wide band UHF array on a flying wing," Proceedings of the 2012 IEEE International Symposium on Antennas and Propagation, Chicago, IL, 2012, pp. 1-2. doi: 10.1109/APS.2012.6348921

[16]. R. Gunnarsson, T. Martin and A. Ouacha, "Wide-band circular antenna arrays consisting of bicone, semi bicone or bowtie elements," 2006 Asia-Pacific Microwave Conference, Yokohama, 2006, pp. 2074-2077. doi: 10.1109/APMC.2006.4429821

[17]. A. Patrovsky and R. Sekora, "Structural integration of a thin conformal annular slot antenna for UAV applications," 2010 Loughborough Antennas & Propagation Conference, Loughborough, 2010, pp. 229-232. doi: 10.1109/LAPC.2010.5666169